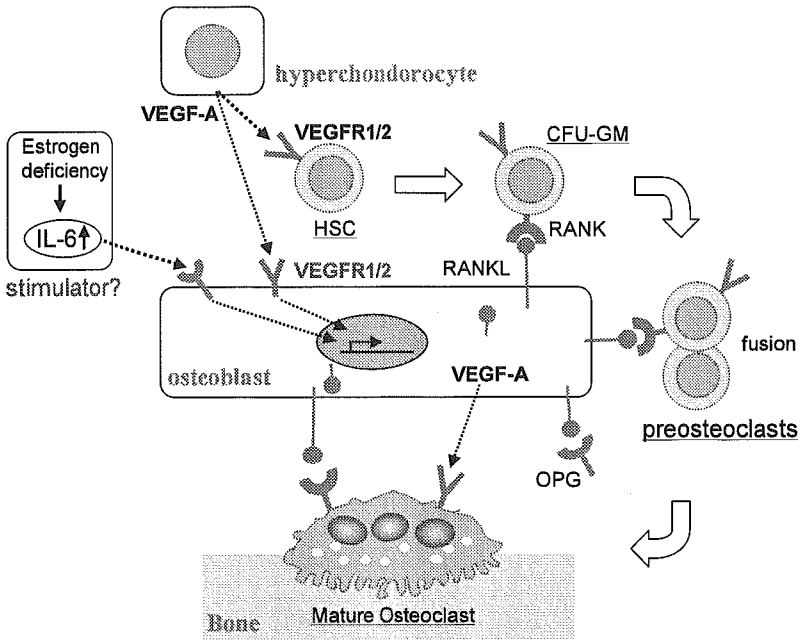

Fig. 7 : Proposed model of VEGF action in osteoclastogenesis. VEGF is produced by hyperchondrocytes and osteoblasts. OPG : osteoprotegerin, HSC : hematopoietic stem cells, CFU : GM : granulocyte : macrophage colony : forming unit.

$VEGF^{120/120}$ mice have a significantly reduced number of osteoclasts. These results indicate that the heparin : binding type of VEGF : A is an important regulator of endochondral ossification. Subsequently, it was shown that mice exclusively expressing $VEGF_{188}$: $VEGF^{188/188}$: also exhibit several bone anomalies. Taken together, these results suggest a crucial role for $VEGF_{164}$ during bone development[61]. It has been reported that no bone anomalies are observed in $VEGF^{164/164}$ mice[61].

: VEGF may contribute to bone formation via a direct effect on osteoblasts. In vitro studies demonstrate that $rhVEGF_{165}$ binds to osteoblasts and stimulates migration, accumulation of PTH : dependent cAMP and upregulation of alkaline phosphatase activity[62]. Several studies demonstrated the expression of VEGFR1 and VEGFR2 on osteoblasts[63]. $VEGF^{120/120}$ mice exhibit reduced osteoblast activity in endochondral bone and intramembranous bone[60]. VEGF : A appears to have multiple functions during bone development.

Conclusions and Future Perspectives

: We have demonstrated that VEGF and PlGF can induce osteoclastogenesis and substitute for CSF : 1 function : Fig. 7 :. Several other studies support our findings[45,57,60]. In addition, we have demonstrated the possibility that VEGF is implicated in estrogen deficiency : dependent bone loss. Although osteoclasts and their precursor cells express VEGFR1 and VEGFR2, our recent experiments suggest that VEGFR1 plays a predominant role in osteoclastogenesis : unpublished data :. However, several questions remain. VEGFR1 signaling is extremely weak. How such a weakly signaling receptor can play a critical role in osteoclastogensis is unclear. This is likely to be addressed in future studies.

: Gene targeting strategies have revealed roles for VEGF in bone development. VEGF is required for angiogenesis and cartilage matrix resorption during endochondral ossification. Taken together with our

findings, these results suggest a critical role for VEGF-mediated blood vessel invasion in coupling cartilage resorption with bone formation, and provide new insights into the regulation of bone development and remodeling.

Acknowledgements

The author thanks the all collaborators for their support and encouragement. This work was supported in part by a Grants-in-Aid from the Ministry of Education, Culture, Sports, Science and Technology of Japan, a grant from Kanzawa Medical Research Foundation, a Research Grant for Longevity Science (14A-2), and a Health and Labor Sciences Research Grant (Research on Dementia and Fracture) from the Ministry of Health, Labor and Welfare of Japan. The author is also grateful for the Lion Award from the Japanese Association for Oral Biology (JAOB) sponsored by the Lion Corporation.

References

1 (Tanaka, S., Takahashi, N., Udagawa, N., Tamura, T., Akatsu, T., Stanley, E. R., Kurokawa, T. and Suda, T. (Macrophage colony-stimulating factor is indispensable for both proliferation and differentiation of osteoclast precursors. J. Clin. Invest. 91 (257 (263, 1993.

2 (Felix, R., Hofsteller, W., Wetterwarld, A., Cecchini, M. G. and Fleisch, H. (Role of colony-stimulating factor-1 in bone metabolism. J. Cell. Biochem. 55 (340 (349, 1994.

3 (Kondo, K., Hiratsuka, S., Subbalakshmi, H., Matsushime, H. and Shibuya, M. (Genomic organization of the flt-1 gene encoding for vascular endothelial growth factor (VEGF (receptor-1 suggests an intimate evolutionary relationship between the 7-Ig and the 5-Ig tyrosine kinase receptors. Gene 208 (297 (305, 1998.

4 (Wiktor-Jedrzejczak, W., Ahmed, A., Szczylik, C. and Skelly, R. R. (Hematological characterization of congenital osteopetrosis in op-op mouse. J. Exp. Med. 156 (1516 (1527, 1982.

5 (Felix, R., Cecchini, M. G., Hofsteller, W., Elford, P. R., Stutzer, A. and Fleisch, H. (Impairment of macrophage colony-stimulating factor production and lack of resident bone marrow macrophages in the osteopetrotic op-op mouse. J. Bone Miner. Res. 5 (781 (789, 1990.

6 (Wiktor-Jedrzejczak, W., Bartocci, A., Ferrante, A. W., Jr., Ahmed-Ansari, A., Sell, K. W., Pollard, J. W. and Stanley, E. R. (Total absence of colony-stimulating factor 1 in the macrophage-deficient osteopetrotic (op-op) mouse. Proc. Natl. Acad. Sci. U. S. A. 87 (4828 (4832, 1990.

7 (Yoshida, H., Hayashi, S. I., Kunisada, T., Ogawa, M., Nishikawa, S., Okamura, H., Sudo, T., Schultz, L. D. and Nishikawa, S. I. (The murine mutation osteopetrosis is in the cording region of the macrophage colony stimulating factor gene. Nature 345 (442 (444, 1990.

8 (Felix, R., Cecchini, M. G. and Fleisch, H. (Macrophage colony-stimulating factor restores in vivo bone resorption in the op-op osteopetrotic mouse. Endocrinology 127 (2592 (2594, 1990.

9 (Kodama, H., Yamasaki, A., Nose, M., Niida, S., Ohgame, Y., Abe, M., Kumegawa, M. and Suda, T. (Congenital osteoclast deficiency in osteopetrotic (op-op) mice is cured by injections of macrophage colony-stimulating factor. J. Exp. Med. 173 (269 (272, 1991.

10 (Wiktor-Jedrzejczak, W., Urbanowska, E., Aukerman, S. L., Pollard, J. W., Stanley, E. R., Ralph, P., Ansari, A. A., Sell, K. W. and Szperl, M. (Correction by CSF-1 of defects in the osteopetrotic op-op mouse suggests local, developmental, and humoral requirements for this growth factor. Exp. Hematol. 19 (1049 (1054, 1991.

11 (Kodama, H., Nose, M., Niida, S. and Yamasaki, A. (Essential role of macrophage colony-stimulating factor in the osteoclast differentiation supported by stromal cells. J. Exp. Med. 173 (1291 (1294, 1991

12 (Hofstetter, W., Wetterwald, A., Cecchini, M. G., Felix, R., Fleisch, H. and Mueller, C. (Detection of transcripts for the receptor for macrophage colony-stimulating factor, c-fms, in murine osteoclast. Proc. Natl. Acad. Sci. U. S. A. 89 (9637 (9641, 1992.

13 (Kodama, H., Yamasaki, A., Abe, M., Niida, S., Hakeda, Y. and Kumegawa, M. (Transient recruitment of osteoclasts and expression of their function in osteopetrotic (op-op) mice by a single injection of macrophage colony-stimulating factor. J. Bone Miner. Res. 8 (45 (50, 1993.

14 (Niida, S., Amizuka, N., Hara, E., Ozawa, E. and Kodama, H. (Expression of Mac-2 antigen in the preosteoclast and osteoclast identified in the op-op

mouse injected with macrophage colony・stimulating factor. J. Bone Miner. Res. 9・873・881, 1994.
15・Wiktor・Jedrzejczak, W., Urbanowska, E. and Szperl, M.・Granulocyte・macrophage colony・stimulating factor corrects macrophage deficiencies, but not osteopetrosis, in the colony・stimulating factor・1・deficient op・op mouse. Endocrinology 134・1932・1935, 1994.
16・Nilsson, S. K., Lieschke, G. J., Garcia・Wijnen, C. C., Williams, B., Tzelepis, D., Hodgson, G., Grail, D., Dunn, A. R. and Bertoncello, I.・Granulocyte・macrophage colony・stimulating factor is not responsible for the correction of hematopoietic deficiencies in the maturing op・op mice. Blood 86・66・72, 1995.
17・Niida, S., Kaku, M., Amano, H., Yoshida, H., Kataoka, H., Nishikawa, S., Tanne, K., Maeda, N., Nishikawa, S. I. and Kodama, H.・Vascular endothelial growth factor can substitute for macrophage colony・stimulating factor in the support of osteoclastic bone resorption. J. Exp. Med. 190・293・298, 1999.
18・Kaku, M., Niida, S., Kawata, T., Maeda, N. and Tanne, K.・Dose・and time・dependent changes in osteoclast induction after a single injection of vascular endothelial growth factor in osteopetrotic mice. Biomed. Res. 21・67・72, 2000.
19・Ferrara, N. and Davis・Smyth, T.・The biology of vascular endothelial growth factor. Endocr. Rev. 18・4・25, 1997.
20・Dvorak, H. F., Brown, L. F., Detmar, M. and Dvorak, A. M.・Vascular permeability factor・vascular endothelial growth factor, microvascular hyperpermeability, and angiogenesis. Am. J. Pathol. 146・1029・1039, 1995.
21・Ogawa, S., Oku, A., Sawano, A., Yamaguchi, S., Yazaki, Y. and Shibuya, M.・A novel type of vascular endothelial growth factor, VEGF・E・NZ・7 VEGF・, preferentially utilizes KDR・Flk・1 receptor and carries a potent mitotic activity without heparin・binding domain. J. Biol. Chem. 273・31273・31282, 1998.
22・Leung, D. W., Cachianes, G., Kuang, W. J., Goeddel, D.・V. and Ferrara, N.・Vascular endothelial growth factor is a secreted angiogenic mitogen. Science 246・1306・1309, 1989.
23・Houck, K. A., Ferrara, N., Winer, J., Cachianes, G., Li, B. and Leung, D. W.・The vascular endothelial growth factor family・identification of a fourth molecular species and characterization of alternative splicing of RNA. Mol. Endocrinol. 5・1806・1814, 1991.
24・Tischer, E., Mitchell, R., Hartman, T., Silva, M., Gospodarowicz, D., Fiddes, J. C. and Abraham, J. A.・The human gene for vascular endothelial growth factor. Multiple protein forms are encoded through alternative splicing. J. Biol. Chem. 266・11947・11954, 1991.
25・Conn, G., Bayne, M. L., Soderman, D. D., Kwok, P.・W., Sullivan, K. A., Palisi, T. M., Hope, D. A. and Thomas, K. A..・Amino acid and cDNA sequences of a vascular endothelial cell mitogen that is homologous to platelet・derived growth factor. Proc. Natl. Acad. Sci. U. S. A. 87・2628・2632, 1990.
26・Houck, K. A., Leung, D. W., Rowland, A. M., Winer, J. and Ferrara, N.・Dual regulation of vascular endothelial growth factor bioavailability by genetic and proteolytic mechanisms. J. Biol. Chem. 267・26031・26037, 1992.
27・Poltorak, Z., Cohen, T., Sivan, R., Kandelis, Y., Spira, G., Voldavsky, I., Keshet, E. and Neufeld, G.・VEGF145, a secreted vascular endothelial growth factor isoform that binds to extracellular matrix. J. Biol. Chem. 272・7151・7158, 1997.
28・Jingjing, L., Xue, Y., Agarwal, N. and Roque, R. S.・Human Muller cells express VEGF183, a novel spliced variant of vascular endothelial growth factor. Invest. Ophthalmol. Vis. Sci. 40・752・759, 1999.
29・Shibuya, M., Yamaguchi, S., Yamane, A., Ikeda, T., Tojo, A., Matsushime, H. and Sato, M.・Nucleotide sequence and expression of a novel human receptor・type tyrosine kinase・flt・closely related to the fms family. Oncogene 5・519・527, 1990.
30・Terman, B. I., Carrion, M. E., Kovacs, E., Rasmussen, B. A., Eddy, R. L. and Shows, T. B.・Identification of a new endothelial cell growth factor receptor tyrosine kinase. Oncogene 6・1677・1683, 1991.
31・Shibuya, M.・Vascular endothelial growth factor receptor family genes・When did the three genes phylogenetically segregate?. Biol. Chem. 383・1573・1579, 2002.
32・Shibuya, M.・Vascular endothelial growth factor receptor・2・its unique signaling and specific ligand, VEGF・E. Cancer Sci. 94・751・756, 2003.
33・De Vries, C., Escobedo, J. A., Ueno, H., Houck, K., Ferrara, N. and Williams, L. T.・The fms・like tyrosine kinase, a receptor for vascular endothelial growth factor. Science 255・989・991, 1992.
34・Hiratsuka, S., Minowa, O., Kuno. J., Noda, T. and Shibuya, M.・Flt・1 lacking the tyrosine kinase domain is sufficient for normal development and angi-

ogenesis in mice. Proc. Natl. Acad. Sci. U. S. A. 95 : 9349 : 9354, 1998.

35 : Kendall, R. L. and Thomas, K. A. : Inhibition of vascular endothelial growth factor activity by an endogenously encoded soluble receptor. Proc. Natl. Acad. Sci. U. S. A. 90 : 10705 : 10709, 1993.

36 : Terman, B. I., Dougher'Vermazen, M., Carrion, M. : E., Dimitrov, D., Armellino, D. C., Gospodarowicz, D. and Bohlen, P. : Identification of KDR tyrosine kinase as a receptor for vascular endothelial growth factor. Biochem. Biophys. Res. Commun. 187 : 1579 : 1586, 1992.

37 : Shalaby, F., Rossant, J., Yamaguchi, T. P., Gertsenstein, M., Wu, X'F., Breitman, M. L. and Schuh, A. C. : Failure of blood'island formation and vasculogenesis in Flk'1'deficient mice. Nature 376 : 62 : 66, 1995.

38 : Carmeliet, P., Ferreira, V., Breier, G., Pollefeyt, S., Kieckens, L., Gertsenstein, M., Fahrig, M., Vandenhoeck, A., Harpal, K., Eberhardt, C., Declercq, C., Pawling, J., Moons, L., Collen, D., Risau, W. and Nagy, A. : Abnormal blood vessel development and lethality in embryos lacking a single VEGF allele. Nature 380 : 435 : 439, 1996.

39 : Ferrara, N., Carver'Moore, K., Chen, H., Dowd, M., Lu, L., O'Shea, K. S., Powell'Braxton, L., Hillan, K. : J. and Moore, M. W. : Heterozygous embryonic lethality induced by targeted inactivation of the VEGF gene. Nature 380 : 439 : 442, 1996.

40 : Soker, S., Takashima, S., Miao, H. Q., Neufeld, G. and Klagsbrun, M. : Neuropilin'1 is expressed by endothelial and tumor cells as an isoform'specific receptor for vascular endothelial growth factor. Cell 92 : 735 : 745, 1998.

41 : Barleon, B., Sozzani, S., Zhou, D., Weich, H. A., Martovani, A. and Marme, D. : Migration of human monocytes in response to vascular endothelial growth factor : VEGF : is mediated via the VEGF receptor flt'1. Blood 87 : 3336 : 3343, 1996.

42 : Clauss, M., Weicht, H., Breier, G., Knies, U., Rockl, W., Waltenberger, J. and Risau, W. : The vascular endothelial growth factor receptor Flt'1 mediates biological activities. J. Biol. Chem. 271 : 17629 : 17634, 1996.

43 : Neufeld, G., Cohen, T., Gengrinovitch, S. and Poltrak, Z. : Vascular endothelial growth factor : VEGF : and its receptors. FASEB J. 13 : 9 : 22, 1999.

44 : Park, J. E., Chen, E. E., Winer, J., Houck, K. A. and Ferrara, N. : Placenta growth factor. Potentiation of vascular endothelial growth'factor bioactivity, in vitro and in vivo, and high affinity binding to Flt'1 but not to Flk'1'KDR. J. Biol. Chem. 169 : 25646 : 25654, 1994.

45 : Nakagawa, M., Kaneda, T., Arakawa, T., Morita, S., Sato, T., Yomada, T., Hanada, K., Kumegawa, M. and Hakeda, Y. : Vascular endothelial growth factor : VEGF : directly enhances osteocalstic bone resorption and survival of mature osteoclasts. FEBS Lett. 473 : 161 : 164, 2000.

46 : Yasuda, H., Shima, N., Nakagawa, N., Yamaguchi, K., kinosaki, M., Mochizuki, S., Tomoyasu, A., Yano, K., Goto, M., Murakami, A., Tsuda, E., Morinaga, T., Higashio, K., Udagawa, N., Takahashi, N. and Suda, T. : Osteoclast differentiation factor is a ligand for osteoprotegerin'osteoclastogenesis'inhibitory factor and is identical to TRANCE'RANKL. Proc. Natl. Acad. Sci. U. S. A. 95 : 3597 : 3602, 1998.

47 : Suda, T., Takahashi, N., Udagawa, N., Jimi, E., Gillespie, M. T. and Martin, T. J. : Modulation of osteoclast differentiation and function by the new members of the tumor necrosis factor receptor and ligand families. Endcr. Rev. 20 : 345 : 357, 1999.

48 : Manolagas, S. C. : Birth and death of bone cells : basic regulatory mechanisms and implications for the pathogenesis and treatment of osteoporosis. Endocr. Rev. 21 : 115 : 137, 2000.

49 : Pacifici, R. : Estrogen, cytokines, and pathogenesis of postmenopausal osteoporosis. J. Bone Miner. Res. 11 : 1043 : 1051, 1996.

50 : Lam, J., Takeshita, S., Barker, J. E., Kanagawa, O., Ross, F. P. and Teitelbaum, S. L. : TNF' : induces osteoclastogenesis by direct stimulation of macrophages exposed to permissive levels of RANK ligand. J. Clin. Invest. 106 : 1481 : 1488, 2000.

51 : Kobayashi, K., Takahashi, N., Jimi, E., Udagawa, N., Takami, M., Kotake, S., Nakagawa, N., Kinosaki, M., Yamaguchi, K., Shima, N., Yasuda, H., Morinaga, T., Higashio, K., Martin, T. J. and Suda, T. : Tumor necrosis factor alpha stimulates osteoclast differentiation by a mechanism independent of the ODF'RANKL' RANK interaction. J. Exp. Med. 191 : 275 : 286, 2000.

52 : Kodama, I., Niida, S., Sanada, M., Yoshiko, Y., Tsuda, M., Maeda, N. and Ohama, K. : Estrogen regulates the production of VEGF for osteoclast formation and activity in op'op mice. J. Bone Miner. Res. 19 : 200 : 206, 2004.

53 : Goad, D. L., Rubin, J., Wang, H., Tashjian, A. H., Jr. and Patterson, C. : Enhanced expression of vascular

endothelial growth factor in human SaOS・2 osteoblast・like cells and murine osteoblasts induced by insulin・like growth factor I. Endocrinology 137・2262・2268, 1996.

54・Steinbrech, D., Mehrara, B., Saddeh, P., Greenwald, J., Spector, J., Gittes, G. and Longaker, M.・VEGF expression in an osteoblast・like cell line is regulated by a hypoxia response mechanism. Am. J. Physiol. Cell Physiol. 278・C853・C860, 2000.

55・Minchenko, A., Bauer, T., Salceda, S. and Caro, J.・Hypoxic stimulation of vascular endothelial growth factor expression in vivo and in vitro. Lab. Invest. 71・374・379, 1994.

56・Pohl, U., Wagner, K. and de Wit, C.・Endothelium・derived nitric oxide in the control of tissue perfusion and oxygen supply・Physiological and pathophysiological implications. Eur. Heart J. 14・93・98, 1993.

57・Gerber, H. P., Vu, T. H., Ryan, A. M., Kowalski, J., Werb, Z. and Ferrara, N.・VEGF couples hypertrophic cartilage remodeling, ossification and angiogenesis during endochondral bone formation. Nat. Med. 5・623・628, 1999.

58・Carlevaro, M. F., Cermelli, S., Cancedda, R. and Cancedda, F. D.・Vascular endothelial growth factor・VEGF・in cartilage neovascularization and chondrocyte differentiation・auto・paracrine role duringendochondral bone formation. J. Cell Sci. 113・59・69, 2000.

59・Haigh, J. J., Gerber, H. P., Ferrara, N. and Wagner, E. F.・Conditional inactivation of VEGF・A in areas of collagen2a1 expression results in embryonic lethality in the heterozygous state. Development 127・5519・5523, 2000.

60・Zelzer, E., McLean, W., Ng, Y・S., Fukai, N., Reginato, A. M., Lovejoy, S., D'Amore, P. A. and Olsen, B. R.・Skeletal defects in $VEGF^{120/120}$ mice reveal multiple roles for VEGF in skeketogenesis. Development 129・1893・1904, 2002.

61・Maes, C., Stockmans, I., Moermans, K., Van Looveren, R., Smets, N., Carmeliet, P., Bouillon, R. and Carmeliet, G.・Soluble VEGF isoforms are essential for establishing epiphyseal vasularization and regulating chondrocyte development and survival. J. Clin. Invest. 113・188・199, 2004.

62・Midy, V. and Plouet, J.・Vasculotropin・vascular endothelial growth factor induces differentiation in cultured osteoblasts. Biochem. Biophys. Res. Commun. 199・380・386, 1994.

63・Deckers, M. M., Karperien, M., van der Bent, C., Yamashita, T., Papapoulos, S. E. and Lowik, C. W.・Expression of vascular endothelial growth factor and their receptors during osteoblast differentiation. Endocrinology 141・1667・1674, 2000.

c-Fos protein as a target of anti-osteoclastogenic action of vitamin D, and synthesis of new analogs

Hisashi Takasu,[1,2] Atsuko Sugita,[2] Yasushi Uchiyama,[2] Nobuyoshi Katagiri,[1] Makoto Okazaki,[2] Etsuro Ogata,[3] and Kyoji Ikeda[1]

[1]Department of Bone and Joint Disease, Research Institute, National Center for Geriatrics and Gerontology, Obu, Japan. [2]Pharmaceutical Research Laboratory, Chugai Pharmaceutical Co. Ltd., Gotemba, Japan. [3]Cancer Institute Hospital, Japanese Foundation for Cancer Research, Tokyo, Japan.

Although active vitamin D drugs have been used for the treatment of osteoporosis, how the vitamin D receptor (VDR) regulates bone cell function remains largely unknown. Using osteoprotegerin-deficient mice, which exhibit severe osteoporosis due to excessive receptor activator of NF-κB ligand/receptor activator of NF-κB (RANKL/RANK) stimulation, we show herein that oral treatment of these mice with 1α,25-dihydroxyvitamin D_3 [1α,25$(OH)_2D_3$] inhibited bone resorption and prevented bone loss, suggesting that VDR counters RANKL/RANK signaling. In M-CSF–dependent osteoclast precursor cells isolated from mouse bone marrow, 1α,25$(OH)_2D_3$ potently and dose-dependently inhibited their differentiation into multinucleate osteoclasts induced by RANKL. Among signaling molecules downstream of RANK, 1α,25$(OH)_2D_3$ inhibited the induction of c-Fos protein after RANKL stimulation, and retroviral expression of c-Fos protein abrogated the suppressive effect of 1α,25$(OH)_2D_3$ on osteoclast development. By screening vitamin D analogs based on their c-Fos–suppressing activity, we identified a new analog, named DD281, that inhibited bone resorption and prevented bone loss in ovariectomized mice, more potently than 1α,25$(OH)_2D_3$, with similar levels of calcium absorption. Thus, c-Fos protein is an important target of the skeletal action of VDR-based drugs, and DD281 is a bone-selective analog that may be useful for the treatment of bone diseases with excessive osteoclastic activity.

Introduction

Excessive osteoclastic bone resorption plays a central role in the pathogenesis of age-related bone loss and microstructural deterioration, leading to fragility fractures (1). Mutinucleated osteoclasts are generated from hematopoietic precursor cells through the action of M-CSF and receptor activator of NF-κB ligand (RANKL) (2–4). These cytokines are produced by osteoclastogenesis-supporting marrow stromal cells and act on osteoclast precursor cells that express their receptors, c-fms and receptor activator of NF-κB (RANK), respectively. These cell-surface receptors transmit osteoclastogenic signals through intracellular kinase cascades that culminate in the activation of transcription factors c-Fos/AP-1 and NF-κB in the nucleus. Accordingly, mice deficient in c-Fos, NF-κB, RANK, RANKL, or M-CSF cannot generate osteoclasts and exhibit osteopetrosis (2–4).

Osteoclasts thus formed fuse with one another and mature into multinucleated, functional osteoclasts that undergo cytoskeletal reorganization and produce effector molecules involved in acidification, degradation of matrix proteins, and expression of hormone/cytokine receptors. Disruption of c-Src, chloride channels, proton pump, or cathepsin K results in the generation of osteoclasts with impaired bone-resorbing function (2). Bisphosphonates, currently most widely used for the treatment of osteoporosis, are known to interfere with the bone-resorbing activity of mature osteoclasts rather than with their differentiation from hematopoietic precursors (5, 6), although the precise target molecules remain to be identified.

Vitamin D hormone, acting through the nuclear vitamin D receptor (VDR), has been used to generate osteoclasts, based on its ability to induce RANKL expression in marrow stromal cells; and it is generally recognized as a bone-resorbing agent (3). Contrary to this belief, we previously demonstrated in estrogen-deficient rats and mice with accelerated bone resorption that alfacalcidol, a prodrug metabolized to the natural vitamin D hormone 1α,25-dihydroxyvitamin D_3 [1α,25$(OH)_2D_3$], and its analog ED-71 reduced the number of osteoclasts, thereby potently suppressing bone resorption in vivo (7–9). Osteoclast activation in estrogen deficiency involves diverse mechanisms, including the production of bone-resorbing cytokines in the bone microenvironment (10, 11) in addition to estrogen's direct effect on osteoclasts and their precursors (12). It is, therefore, difficult to identify the target cell and molecule of 1α,25$(OH)_2D_3$ in ovariectomy models. In order to define the molecular pathway(s) that VDR acts upon, we examined the effects of 1α,25$(OH)_2D_3$ in a genetic model of osteoporosis due to constitutive activation of RANK signaling.

Results

1α,25$(OH)_2D_3$ inhibits bone resorption in osteoprotegerin KO mice. Osteoprotegerin (OPG) is a decoy receptor of RANKL that belongs to the TNF receptor family (13), and mice lacking OPG exhibit excessive bone resorption as a result of constitutive activation of RANKL/RANK signaling (14). Oral administration of 1α,25$(OH)_2D_3$ to *OPG* homozygous KO mice caused a dose-dependent reduction in the osteoclast number (Figure 1A) and in osteoclast surface

Nonstandard abbreviations used: BMD, bone mineral density; 1α,25$(OH)_2D_3$, 1α,25-dihydroxyvitamin D_3; OPG, osteoprotegerin; OVX, ovariectomized; RANK, receptor activator of NF-κB; RANKL, RANK ligand; TRAP, tartrate-resistant acid phosphatase; VDR, vitamin D receptor.

Conflict of interest: E. Ogata is a member of the board of Chugai Pharmaceutical Co., which manufactures active vitamin D derivatives for the treatment of bone diseases.

Citation for this article: *J. Clin. Invest.* **116**:528–535 (2006). doi:10.1172/JCI24742.

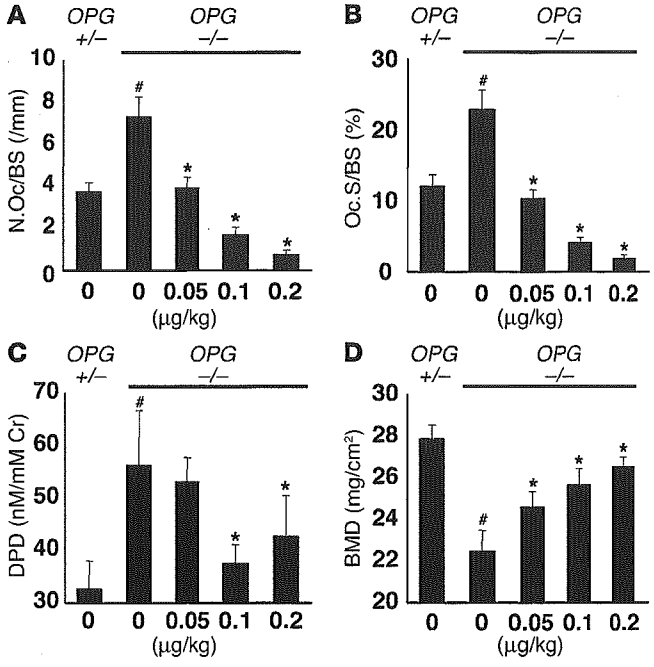

Figure 1
$1\alpha,25(OH)_2D_3$ inhibits bone resorption in *OPG* KO mice. *OPG* homozygous KO (–/–) mice were treated orally with the indicated doses of $1\alpha,25(OH)_2D_3$ for 6 weeks, and osteoclast number (corrected for bone surface; N.Oc/BS (**A**), bone surface covered by osteoclasts (Oc.S/BS) (**B**), urinary deoxypyridinoline excretion (DPD; corrected for creatinine [Cr]) (**C**), and BMD (**D**) at the left femur were determined as described in Methods. Heterozygous (+/–) littermates served as the control. $^*P < 0.01$ versus *OPG* KO group with vehicle treatment, $^\#P < 0.01$ versus heterozygous control group, $n = 6$ each group.

area (Figure 1B) in bone sections, down to levels in heterozygous mice used as a control. The suppressive effect of $1\alpha,25(OH)_2D_3$ on bone resorption was also demonstrated by a reduction in the urinary level of a biochemical marker of bone resorption, deoxypyridinoline (Figure 1C). As reported previously (14), OPG-deficient mice had a markedly reduced bone mineral density (BMD) as a result of excessive bone resorption, and oral administration of $1\alpha,25(OH)_2D_3$ caused a dose-dependent amelioration of bone loss at the tibia (Figure 1D). The small pharmacological doses of $1\alpha,25(OH)_2D_3$ used in the current study (0.05–0.2 μg/kg) did not induce hypercalcemia (data not shown). These results suggest that $1\alpha,25(OH)_2D_3$ acts as an inhibitor of bone resorption in vivo by countering the RANKL/RANK pathway. In light of our previous observations that the expression of RANKL in bone did not increase following $1\alpha,25(OH)_2D_3$ administration in vivo (9), we hypothesized that $1\alpha,25(OH)_2D_3$ suppresses bone resorption by interfering with signaling through RANK receptors on osteoclast precursor cells.

$1\alpha,25(OH)_2D_3$ inhibits osteoclast development by acting directly on osteoclast precursor cells in bone marrow. In order to examine whether $1\alpha,25(OH)_2D_3$ counters osteoclastogenic signaling emanating from RANK receptors, we isolated osteoclast progenitor cells from mouse bone marrow and examined the effects of $1\alpha,25(OH)_2D_3$ on RANKL-induced osteoclastogenesis. In the presence of M-CSF and RANKL, the murine cultures gave rise to numerous multinucleated giant cells (Figure 2A) that were capable of forming resorption pits on dentine slices (data not shown). Treatment of the same cultures with $1\alpha,25(OH)_2D_3$ resulted in a dose-dependent reduction in the number of osteoclasts formed (Figure 2, A and B). $1\alpha,25(OH)_2D_3$ caused a significant reduction in the osteoclast number at a concentration as low as 10^{-9} M and inhibited the formation of osteoclasts by 70% at 10^{-8} M (Figure 2B).

The whole process of osteoclast development in murine cultures consists mainly of 2 phases: first, a stage of M-CSF–dependent growth of osteoclast progenitors, and then a latter phase of terminal differentiation induced by RANKL in the presence of M-CSF. The former process was assessed by isolation of osteoclast progenitor cells from bone marrow and measurement of their prolifera-

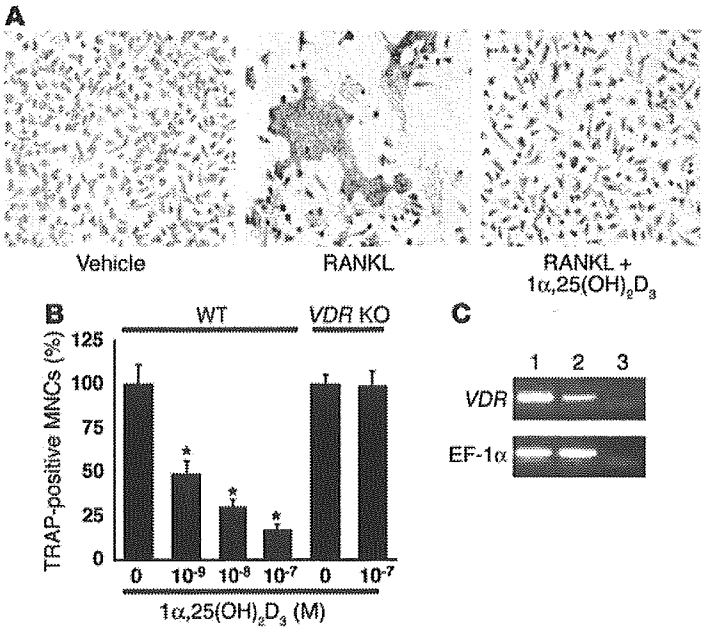

Figure 2
$1\alpha,25(OH)_2D_3$ inhibits osteoclast development through *VDR* by acting directly on osteoclast precursor cells in bone marrow. (A and B) Osteoclast precursor cells were isolated from the bone marrow of WT C57BL/6J and *VDR* KO mice (**B**) as M-CSF–dependent adherent cells, as described in Methods, and were further treated with RANKL (40 ng/ml) in the absence or presence of 10^{-7} M $1\alpha,25(OH)_2D_3$ for 3 days (**A**). Note that the development of TRAP-positive multinucleate osteoclasts induced by RANKL was markedly inhibited by cotreatment with $1\alpha,25(OH)_2D_3$. (**B**) The inhibitory effect of $1\alpha,25(OH)_2D_3$ on the formation of TRAP-positive multinucleate cells (MNCs) was dose-dependent and was not seen in marrow cultures derived from *VDR* KO mice, even at the highest dose of 10^{-7} M. Data are expressed as a percentage of vehicle-treated cultures. $^*P < 0.05$ versus vehicle group, $n = 6$. (**C**) Expression of *VDR*s in the intestine (lane 1) and osteoclast precursor cells (lane 2) as detected by RT-PCR. EF-1α mRNA served as control for PCR. Lane 3 contained water as a negative control.

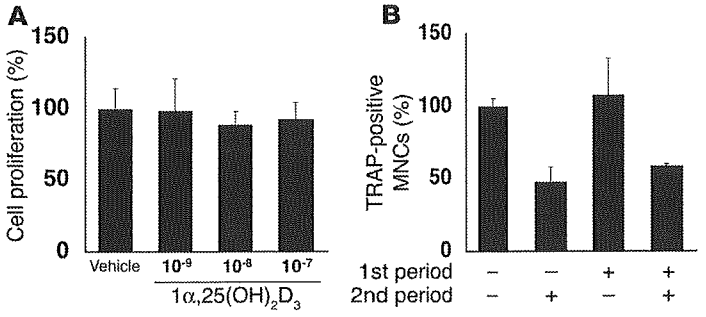

Figure 3

$1\alpha,25(OH)_2D_3$ inhibits RANKL-induced terminal differentiation into osteoclasts. (**A**) Osteoclast precursor cells were isolated from the bone marrow of WT C57BL/6J mice. These cells were cultured in the presence of 30 ng/ml M-CSF without or with increasing doses of $1\alpha,25(OH)_2D_3$ for 3 days, and cell proliferation was assessed as described in Methods. (**B**) Bone marrow cells were cultured with M-CSF for the first 3 days (1st period) and then with RANKL in addition to M-CSF for the latter 3 days (2nd period). The presence of $1\alpha,25(OH)_2D_3$ at 10^{-8} M is indicated by "+". Note that the presence of $1\alpha,25(OH)_2D_3$ only in the latter period was sufficient to inhibit the formation of TRAP-positive multinucleate cells, whereas its presence in the former M-CSF–dependent cell growth period failed to inhibit osteoclastogenesis.

tive responses to M-CSF. As shown in Figure 3A, treatment with $1\alpha,25(OH)_2D_3$ between 10^{-9} M and 10^{-7} M did not affect M-CSF–dependent cell proliferation, suggesting that $1\alpha,25(OH)_2D_3$ mainly acts at the latter differentiation stage. Also consistent with this notion are the results that treatment of bone marrow cultures with $1\alpha,25(OH)_2D_3$ only during the latter half (3 days) of the 6-day period was sufficient to inhibit osteoclast formation, whereas its presence in the former half period (3 days) during M-CSF–dependent growth failed to do so (Figure 3B). The presence of $1\alpha,25(OH)_2D_3$ throughout the 6-day culture period did not result in further inhibition of osteoclastogenesis. Thus, although $1\alpha,25(OH)_2D_3$ is well known for its antiproliferative activity in a variety of cell types (15), in this case the RANKL-dependent terminal differentiation step of osteoclast progenitor cells was specifically inhibited by $1\alpha,25(OH)_2D_3$.

When osteoclast precursor cells were isolated from the bone marrow of VDR-deficient mice, the suppressive effect of $1\alpha,25(OH)_2D_3$ on osteoclastogenesis was not observed at all, even at the highest dose of 10^{-7} M (Figure 2B). Taken together with the expression of VDR in the osteoclast precursor cells (Figure 2C), these data indicate that $1\alpha,25(OH)_2D_3$ acts directly on osteoclast precursors and inhibits their differentiation into mature osteoclasts and that this effect is mediated through the VDR.

c-Fos protein as a target of anti-osteoclastogenic action of $1\alpha,25(OH)_2D_3$. In order to clarify the mechanism by which $1\alpha,25(OH)_2D_3$ inhibits osteoclastogenic signaling in precursor cells, we investigated the effects of $1\alpha,25(OH)_2D_3$ on molecules that are known to transmit signals from the RANK receptor. Western blot analysis revealed that $1\alpha,25(OH)_2D_3$ did not affect the protein levels of the RANK receptor itself, TRAF6, p65 and p52 subunits of NF-κB, or c-Jun protein (Figure 4A and data not shown). Stimulation with RANKL caused activation of IκB kinase, p38, and JNK, through their phosphorylation; however, $1\alpha,25(OH)_2D_3$ even at 10^{-7} M did not inhibit their phosphorylation (Figure 4B). In contrast, $1\alpha,25(OH)_2D_3$ did inhibit the induction of c-Fos protein by RANKL in a dose-dependent manner, and this effect on c-Fos protein was not observed in cells derived from *VDR* KO mice (Figure 5A). Treatment with $1\alpha,25(OH)_2D_3$ alone had no effect. These results suggest that $1\alpha,25(OH)_2D_3$ blocked the induction by RANKL of c-Fos protein, a component of the AP-1 transcription factor, thereby antagonizing its transcription function in the nucleus.

Interestingly, the marked reduction in c-Fos protein took place with just a modest change in the level of c-Fos mRNA. Quantification of the c-Fos mRNA level by quantitative RT-PCR analysis revealed a substantial increase following RANKL stimulation, peaking at 6 hours, but $1\alpha,25(OH)_2D_3$ only modestly inhibited this increase in c-Fos mRNA at this time point (Figure 5B), suggesting that a posttranscriptional mechanism is involved in the VDR-mediated suppression of the c-Fos protein. Pulse-chase experiments revealed that c-Fos protein in osteoclast precursor cells turned over rapidly with an estimated half-life of less than 2 hours, as reported for other cell types (16), whereas treatment with $1\alpha,25(OH)_2D_3$ did not result in a further acceleration of c-Fos degradation (Figure 6, A and B). In pulse-labeling experiments, biosynthesis of c-Fos protein, which increased markedly after RANKL stimulation, was inhibited by cotreatment with $1\alpha,25(OH)_2D_3$ (Figure 6C).

Earlier targeted gene ablation experiments revealed a fundamental role of the Fos/AP-1 transcription factor in osteoclast development (17, 18), and recent studies identified its critical target molecules (19–21). As reported, stimulation with RANKL induced 2 notable c-Fos target genes, NFATc1 and IFN-β, which regulate osteoclast differentiation positively and negatively, respectively (Figure 7A). Simultaneous treatment with $1\alpha,25(OH)_2D_3$ inhibited the induction of these target molecules of the c-Fos transcription factor (Figure 7A); this finding can be taken as evidence that $1\alpha,25(OH)_2D_3$, by suppressing the level of c-Fos protein, functionally dampens its transcription activity. Thus, it is conceivable that suppression of c-Fos protein plays an important role in the functional interference of $1\alpha,25(OH)_2D_3$ with osteoclastogenesis.

In order to prove that $1\alpha,25(OH)_2D_3$-mediated inhibition of c-Fos protein induction by RANKL was responsible for the suppressive effect of the hormone on osteoclast differentiation, we transfected osteoclast precursor cells with a retroviral vector encoding c-Fos protein and then examined them for the ability of $1\alpha,25(OH)_2D_3$ to suppress osteoclast formation. Forced expression of c-Fos protein abrogated the suppressive effect of $1\alpha,25(OH)_2D_3$ on osteoclastogenesis completely at 10^{-9} M and partially at 10^{-8} M (Figure 7B).

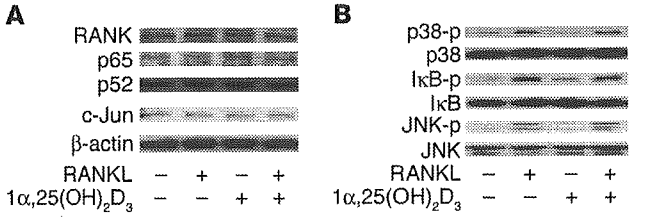

Figure 4

$1\alpha,25(OH)_2D_3$ fails to inhibit NF-κB and p38/JNK pathways in osteoclast precursor cells. Osteoclast precursor cells were isolated from the bone marrow of C57BL/6J mice as M-CSF–dependent adherent cells and were treated with RANKL (40 ng/ml) for 24 hours in the absence or presence of 10^{-8} M $1\alpha,25(OH)_2D_3$. Expression of RANK, p65, p52, and c-Jun proteins (**A**) and phosphorylation of IκB (IκB-p), p38 (p38-p), and JNK (JNK-p) (**B**) were analyzed by Western blotting after RANKL treatment for 15 minutes. β-Actin protein served as a loading control.

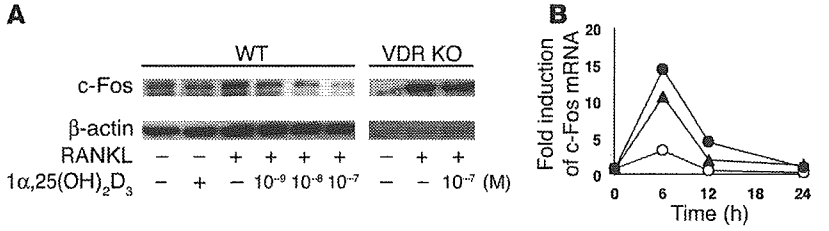

Figure 5
$1\alpha,25(OH)_2D_3$ inhibits expression of c-Fos protein induced by RANKL. Osteoclast precursor cells were isolated from the bone marrow of WT C57BL/6J and *VDR* KO mice as M-CSF–dependent adherent cells and were treated with RANKL (40 ng/ml) for 24 hours in the absence or presence of the indicated doses of $1\alpha,25(OH)_2D_3$. Western blotting for c-Fos protein (**A**) and quantitative RT-PCR analyses (**B**) were performed. RNA was isolated from osteoclast precursor cells at the indicated times after RANKL stimulation, and quantitative RT-PCR for c-Fos mRNA was performed using a LightCycler with EF-1α mRNA as a control. Filled circles, filled triangles, and open circles represent RANKL, RANKL plus $1\alpha,25(OH)_2D_3$, and vehicle, respectively. β-Actin protein served as a loading control (**A**).

Vitamin D analogs that reduce c-Fos protein and inhibit osteoclast differentiation more potently than the natural hormone. The finding that the suppression of c-Fos underlies the anti-osteoclastogenic function of the VDR suggests that the former activity can be used for screening vitamin D analogs for those with more potent antiresorptive function than the natural hormone, $1\alpha,25(OH)_2D_3$. By screening newly synthesized vitamin D compounds, we identified 2 analogs, DD280 and DD281, that reduced the level of c-Fos protein more potently than $1\alpha,25(OH)_2D_3$ (Figure 8, A and B). When the analogs were tested in murine bone marrow cultures, it was evident that, by reducing the level of c-Fos protein, these analogs caused more potent suppression of osteoclast development than the natural hormone (Figure 8C).

We tested one of the potent analogs, DD281, for its pharmacological activity in vivo. The major action of vitamin D hormone is to stimulate intestinal calcium absorption, and its therapeutically beneficial action in bone is often compromised by side effects, such as hypercalcemia and hypercalciuria, especially when the dosage is increased. DD281, which is chemically (1R,3S,5Z)-5-[(2E)-[(3aS,7aS)-1-[(1R)-1-[(2-ethyl-2-hydroxybutyl)thio]ethyl]-3,3a,5,6,7,7a-hexahydro-7a-methyl-4H-inden-4-ylidene]ethylidene]-4-methylene-1,3-cyclohexanediol (Figure 9A), has a binding affinity for the VDR that is approximately 84% of that of $1\alpha,25(OH)_2D_3$; it also has a very short half-life in the circulation [less than 1 hour versus 8–10 hours for $1\alpha,25(OH)_2D_3$ when administered orally], presumably because of its very low affinity for vitamin D–binding protein [0.3% of that of $1\alpha,25(OH)_2D_3$]. We determined the doses of DD281 that had an effect on calcium absorption similar to the effect of $1\alpha,25(OH)_2D_3$ by estimating urinary calcium excretion in ovariectomized (OVX), estrogen-deficient mice. As summarized in Figure 9B, the lower dose of DD281 (5 μg/kg body weight) or $1\alpha,25(OH)_2D_3$ (0.0125 μg/kg body weight) did not change the 24-hour urinary excretion of calcium, whereas the higher dose of each [10 μg/kg for DD281 and 0.05 μg/kg for $1\alpha,25(OH)_2D_3$] caused a similar increase in urinary calcium excretion. For the same degree of effect on calcium metabolism, DD281 prevented bone loss more significantly and more potently than $1\alpha,25(OH)_2D_3$ at the lumbar spine (Figure 9C). Also, DD281 reduced the osteoclast number and the bone surface covered by osteoclasts more significantly and more potently than $1\alpha,25(OH)_2D_3$ at the lumbar spine (Table 1). Neither drug caused hypercalcemia, although the higher dose of $1\alpha,25(OH)_2D_3$ raised serum calcium concentrations slightly but significantly, only when compared with those in vehicle-treated OVX mice (Table 2). Thus, DD281 was superior to $1\alpha,25(OH)_2D_3$ in antiresorptive and bone-protective effects while having the same effect on calcium metabolism as the natural hormone.

Discussion

Hypocalcemia and rickets/osteomalacia observed in VDR gene KO mice as well as in patients with vitamin D deficiency point to the physiological importance of VDR in maintaining calcium homeostasis and bone mineralization (22). Regarding the pharmacology, the importance of vitamin D as a nutrient for the prevention of osteoporosis is well recognized, especially in the elderly population, in which simple vitamin D deficiency is prevalent (23, 24). However, the utility of vitamin D hormone in osteoporotic patients, even in the setting of vitamin D sufficiency, and whether or not it has any peculiar properties in terms of bone action not shown by plain vita-

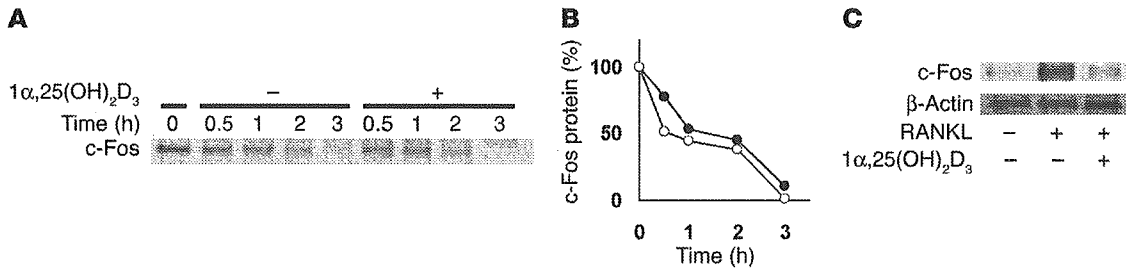

Figure 6
$1\alpha,25(OH)_2D_3$ inhibits translation of c-Fos protein in osteoclast precursor cells. Osteoclast precursor cells were isolated from the bone marrow of C57BL/6J mice as M-CSF–dependent adherent cells. (**A** and **B**) After RANKL stimulation for 24 hours, osteoclast progenitor cells were pulse-labeled for 30 minutes with ^{35}S-methionine followed by chasing with cold methionine for the indicated times in the absence or presence of $1\alpha,25(OH)_2D_3$ treatment. Note that the degradation of c-Fos protein was not accelerated by $1\alpha,25(OH)_2D_3$ (open circles), compared with that for vehicle-treated cells (filled circles). (**C**) After RANKL stimulation for 24 hours, osteoclast progenitor cells were pulse-labeled for 30 minutes with ^{35}S-methionine in the absence or presence of $1\alpha,25(OH)_2D_3$. Labeled c-Fos protein was immunoprecipitated. Note that the biosynthesis of c-Fos protein stimulated by RANKL was inhibited by $1\alpha,25(OH)_2D_3$ treatment. β-Actin protein served as a loading control.

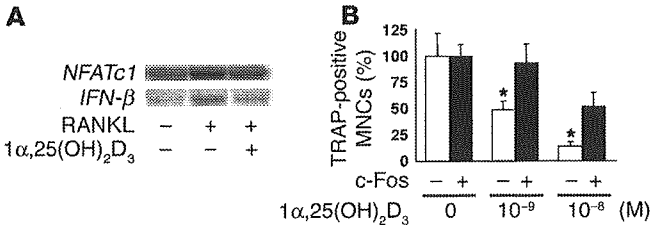

Figure 7
c-Fos protein as a target of anti-osteoclastogenic action of $1\alpha,25(OH)_2D_3$. Osteoclast precursor cells were isolated from the bone marrow of C57BL/6J mice as M-CSF–dependent adherent cells and were treated with RANKL (40 ng/ml) for 24 hours in the absence or presence of the indicated doses of $1\alpha,25(OH)_2D_3$. (**A**) Northern blot analysis of c-Fos target genes, i.e., *NFATc1* and *IFN-β*, in RANKL-treated osteoclast precursor cells without or with $1\alpha,25(OH)_2D_3$ for 24 hours (10^{-7} M). (**B**) Forced expression of c-Fos (indicated by "+") by a retroviral vector abrogated the suppressive effect of $1\alpha,25(OH)_2D_3$ on osteoclast development. Osteoclast precursor cells isolated from bone marrow were infected with a retroviral vector encoding c-Fos, and cultured with M-CSF and RANKL for 3 days in the absence or presence of $1\alpha,25(OH)_2D_3$. Data are expressed as a percentage of the value for vehicle-treated cultures without retroviral infection (–). $^*P < 0.05$ versus vector-infected group, $n = 6$.

min D, has been controversial (25, 26). It is generally believed that $1\alpha,25(OH)_2D_3$ stimulates bone resorption, based on the fact that it was found to be a bone-resorbing hormone in a classic experiment using bone organ cultures (27), and the fact that $1\alpha,25(OH)_2D_3$ induces the expression of RANKL, an essential cytokine for osteoclast development (28). In the present study we have provided biochemical as well as histological evidence that vitamin D hormone can exert a pharmacological action to inhibit bone resorption under pathological conditions with excessive osteoclast generation. The exact reason for these contrasting effects of $1\alpha,25(OH)_2D_3$ on bone resorption is not clear at the present time. $1\alpha,25(OH)_2D_3$ at high concentrations is known to induce the expression of RANKL in stromal/osteoblastic cells in vitro, which is assumed to favor osteoclastogenesis. In sharp contrast, as demonstrated in the current study, $1\alpha,25(OH)_2D_3$ can act on hematopoietic lineage cells and potently inhibit their differentiation into mature osteoclasts. $1\alpha,25(OH)_2D_3$ has also been shown to inhibit osteoclast differentiation from human PBMCs (29). We (7, 8, 30) and others (31) have previously reported that when vitamin D hormone is administered in vivo at pharmacological doses in animal models with excessive bone resorption, it actually reduces osteoclast number and suppresses bone resorption. This has been proven in a recent clinical trial, in which ED-71, a vitamin D analog, reduced a bone resorption marker and increased BMD in osteoporotic patients with native vitamin D_3 supplementation (32). It is conceivable, therefore, that in vivo, the anti-osteoclastogenic action through VDR in hematopoietic cells may outweigh the pro-osteoclastogenic action through stromal cells, leading to a net decrease in bone resorption. In fact, we failed to find an increase in RANKL expression in vivo even when toxic doses of $1\alpha,25(OH)_2D_3$ that induced overt hypercalcemia were administered (9). Others have reported that $1\alpha,25(OH)_2D_3$ within a certain dose range inhibits parathyroid hormone–induced (PTH-induced) RANKL expression in the bones of thyroparathyroidectomized rats (31). Alternatively, under pathological conditions with elevated bone resorption, VDR signaling may be downregulated in stromal/osteoblastic cells, relative to that in hematopoietic cells, which would mask the pro-osteoclastogenic action of vitamin D. Further studies are required to determine the relative contribution of stromal versus hematopoietic cells to the in vivo regulation of bone resorption through the VDR.

The major action of vitamin D is stimulation of intestinal calcium absorption; and the therapeutic effects of vitamin D on bone, whether active or plain vitamin D, are believed to be indirect, through stimulation of intestinal calcium absorption, correction of a negative calcium balance, and normalization of the sustained PTH secretion frequently seen in elderly patients (33). In order to gain some insight into the role of PTH suppression in vitamin D action on bone, we previously examined the effects of $1\alpha,25(OH)_2D_3$ and its analog [22-oxa-$1\alpha,25(OH)_2D_3$] on bone resorption in parathyroidectomized rats rendered hypercalcemic with constant PTH-related protein infusion (34). Under these "PTH clamp" conditions, we observed that $1\alpha,25(OH)_2D_3$ and 22-oxa-$1\alpha,25$-dihydroxyvitamin D_3 were capable of inhibiting bone resorption (34). In agreement with these previous findings, we have demonstrated in this study that vitamin D hormone acts directly on hematopoietic cells in bone marrow, through VDR expressed in osteoclast progenitors of the monocyte/macrophage lineage, thereby inhibiting their terminal differentiation into mature osteoclasts. Thus, hematopoietic cells that receive the RANKL signal through the RANK receptor are important target cells of vitamin D action in vivo.

We further investigated the mechanism by which $1\alpha,25(OH)_2D_3$ modulates the developmental program of hematopoietic precursor cells and inhibits their differentiation into mature osteoclasts. This process is tightly regulated by extracellular signals, including RANKL as an essential cytokine, as well as by negative regulators, such as OPG and other inhibitory molecules (35, 36). Our find-

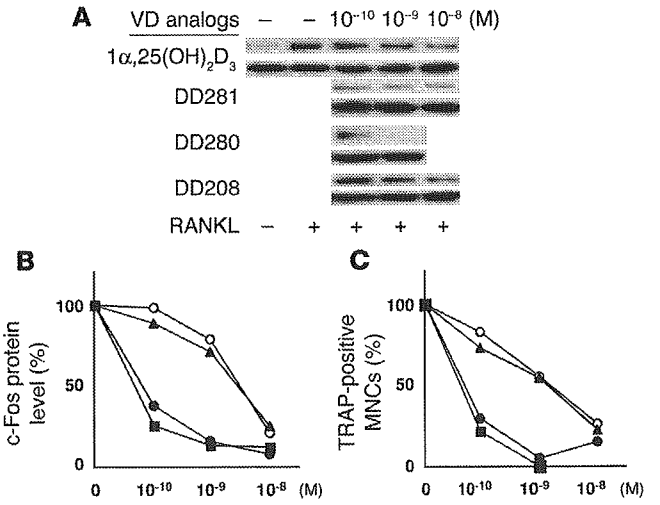

Figure 8
Screening for vitamin D (VD) analogs that reduce c-Fos protein and inhibit osteoclast differentiation more potently than $1\alpha,25(OH)_2D_3$. The effects of $1\alpha,25(OH)_2D_3$ (open circles) and its analogs (DD281, DD280, and DD208) on the c-Fos protein level in osteoclast precursor cells (**A** and **B**) and the formation of TRAP-positive multinucleate osteoclasts (**C**) at the indicated concentrations are shown. The lower bands in **A** show β-actin as an internal control for protein loading. Filled circles, rectangles, and triangles (**B** and **C**) represent DD281, DD280, and DD208, respectively. Data are expressed as a percentage of the value for vehicle-treated cultures.

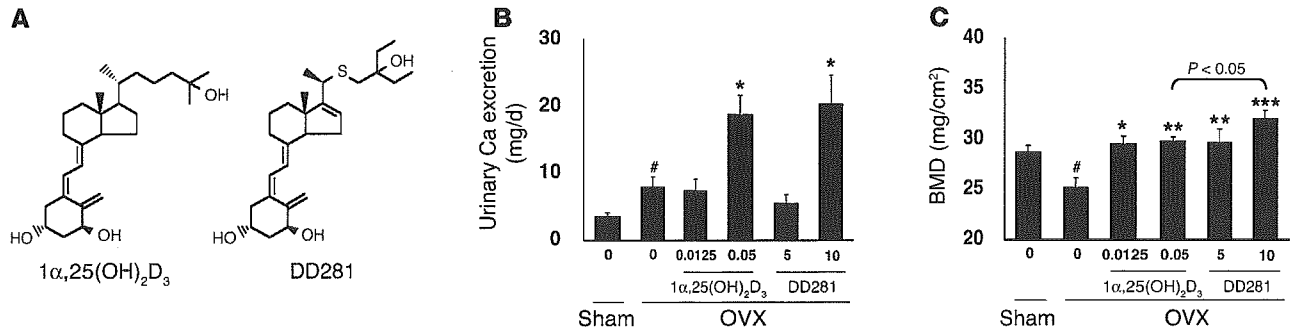

Figure 9

A novel vitamin D analog, DD281, inhibits osteoclast differentiation and increases BMD more potently than $1\alpha,25(OH)_2D_3$ in vivo. (**A**) Structures of $1\alpha,25(OH)_2D_3$ and its analog, DD281. (**B**) Ovariectomized (OVX) C57BL/6J mice were treated orally with the indicated doses of $1\alpha,25(OH)_2D_3$ or its analog DD281 for 4 weeks, and urinary calcium excretion was determined for the final 24 hours. $^*P < 0.05$ versus OVX group with vehicle treatment, $^{\#}P < 0.05$ versus sham group, $n = 8$ each group. (**C**) BMD at the lumbar vertebrae was determined. $^*P < 0.05$ versus OVX group with vehicle treatment, $^{**}P < 0.005$ versus OVX group with vehicle treatment, $^{***}P < 0.0005$ versus OVX group with vehicle treatment, $^{\#}P < 0.05$ versus sham group, $n = 8$ each group.

ings that $1\alpha,25(OH)_2D_3$ inhibited bone resorption in mice lacking OPG rule out the possibility that the antiresorptive action is mediated through OPG. It is also unlikely that $1\alpha,25(OH)_2D_3$ interferes with the binding of RANKL to its receptor RANK and inhibits its overall signaling, since some intracellular signals activated downstream of RANK, such as IκB kinase and JNK, were not affected by $1\alpha,25(OH)_2D_3$. Instead, our data suggest that, among known signaling molecules involved in osteoclast development downstream of the RANK receptor, c-Fos protein is a key target molecule of VDR. In addition, our experiments revealed that the reduction in the level of c-Fos protein took place with only a modest decrease in its mRNA level. Taken together with the results of the pulse-labeling experiments, this finding suggests that VDR, classically viewed as a transcription factor, inhibits the translation of c-Fos protein, although the underlying molecular mechanism remains elusive. The effect of $1\alpha,25(OH)_2D_3$ on c-Fos protein in osteoclast precursors contrasts with the reported effect of $1\alpha,25(OH)_2D_3$ on c-Fos gene transcription in osteoblasts and other cell types (37, 38). Thus, there may exist cell type–specific regulatory mechanisms that modulate the expression of c-Fos gene expression in response to $1\alpha,25(OH)_2D_3$. Since a number of other proteins involved in RANK signaling, such as RANK itself, JNK, p38 MAPK, IκB kinase, p65 and p52 subunits of NF-κB, and c-Jun, were not affected by $1\alpha,25(OH)_2D_3$, it is conceivable that the inhibitory effect of the VDR is specific to c-Fos protein in osteoclast precursor cells.

Importantly, the suppression of c-Fos protein through VDRs is critical for the pharmacological action of vitamin D, since we showed that forced expression of c-Fos blocked the suppressive effect of vitamin D on osteoclast formation. The identification of novel synthetic vitamin D analogs that were capable of inhibiting osteoclast development more efficiently than the natural hormone, $1\alpha,25(OH)_2D_3$, in parallel with greater suppression of c-Fos protein, lends further support to our concept that c-Fos–suppressing activity is important for the antiresorptive function of vitamin D. This mechanism may also underlie the activity of other recently developed bone-selective vitamin D analogs (39, 40). It should be noted, however, that DD281 was not completely bone-selective and increased urinary calcium excretion above that in the vehicle-treated mice. Therefore, careful monitoring of urinary and serum calcium levels would be required if its clinical utility were to be tested.

In conclusion, we demonstrated herein that the pharmacological action of $1\alpha,25(OH)_2D_3$ is to mitigate excessive bone resorption, under pathological conditions such as osteoporosis; that it does so by acting on monocyte/macrophage-lineage cells in bone marrow; that the presence of VDRs is a prerequisite for this action; and that c-Fos protein is a key target molecule of VDR action. Based on these findings, we synthesized new vitamin D analogs, among which DD281, with potent antiresorptive activity relative to calcium absorption function, may warrant clinical trial for the treatment of bone diseases associated with excessive osteoclastic activity.

Methods

Reagents. $1\alpha,25(OH)_2D_3$ and its analogs, including DD208, DD280, and DD281, were synthesized at Chugai Pharmaceutical Co. Mouse RANKL and M-CSF were purchased from R&D Systems. Antibodies against RANK, TRAF6, p65, and p52 were purchased from Santa Cruz Biotechnology Inc. Anti–c-Jun and –c-Fos antibodies came from Sigma-Aldrich.

Animal experiments. Six-week-old female *OPG* homozygous and heterozygous KO mice were purchased from CLEA Japan Inc. and acclimated for 1 week under standard laboratory conditions at 24 ± 2°C and

Table 1

Effects of $1\alpha,25(OH)_2D_3$ and DD281 on osteoclast parameters in OVX mice

Treatment		$1\alpha,25(OH)_2D_3$		DD281	
Dose (μg/kg body weight)	0	0.0125	0.05	5	10
Oc.S/BS (%)	13.3 ± 0.7	10.5 ± 1.4	11.1 ± 0.4[A]	11.3 ± 0.8	9.8 ± 0.4[B,C]
N.Oc/BS (no./mm)	2.5 ± 0.2	2.2 ± 0.3	2.4 ± 0.2	2.3 ± 0.2	1.8 ± 0.2[A,C]

Eleven-week-old OVX mice ($n = 8$ each group) were treated with $1\alpha,25(OH)_2D_3$ or DD281 at the indicated doses for 4 weeks. Bone histomorphometry was performed at the lumbar spine. Oc.S/BS, bone surface covered by osteoclasts; N.Oc/BS, number of osteoclasts, corrected for bone surface. $^AP < 0.05$ versus OVX group, $^BP < 0.005$ versus OVX group, $^CP < 0.05$ versus $1\alpha,25(OH)_2D_3$-treated group.

Table 2
Blood and urine biochemistry in OVX mice treated with $1\alpha,25(OH)_2D_3$ or DD281

Operation	Sham	OVX				
Treatment	Vehicle	Vehicle	$1\alpha,25(OH)_2D_3$		DD281	
Dose (μg/kg body weight)			0.0125	0.05	5	10
Serum						
Calcium (mg/dl)	9.63 ± 0.13	9.34 ± 0.11	9.09 ± 0.09	9.69 ± 0.09[A]	9.19 ± 0.05	9.31 ± 0.11
Phosphorus (mg/dl)	8.35 ± 0.39	7.50 ± 0.41	6.36 ± 0.24[A]	8.19 ± 0.47	6.39 ± 0.21	7.23 ± 0.19
Urine						
Phosphorus/Creatinine	6.71 ± 0.45	6.74 ± 0.44	7.75 ± 0.32	7.10 ± 0.52	6.28 ± 0.56	6.32 ± 0.32

Eleven-week-old OVX mice (n = 8 per group) were treated with $1\alpha,25(OH)_2D_3$ or DD281 at the indicated doses for 4 weeks. Urine was collected during the final 24 hours, and blood was drawn to obtain serum. [A]$P < 0.05$ versus OVX group.

50–60% humidity. The mice were allowed free access to tap water and commercial standard rodent chow (CE-2) containing 1.20% calcium, 1.08% phosphate, and 240 IU/100 g vitamin D_3 (CLEA Japan Inc.). After acclimation, various doses of $1\alpha,25(OH)_2D_3$ or vehicle (medium chain triglyceride) were administered orally 5 times a week for 6 weeks.

Nine-week-old female C57BL/6J mice were purchased from Japan SLC Inc. and ovariectomized (OVX) after a 1-week acclimation. Sham-operated mice served as the control. OVX mice were treated orally with $1\alpha,25(OH)_2D_3$ (0.0125–0.05 μg/kg body weight once daily), its analog DD281 (5–10 μg/kg body weight twice daily), or vehicle (medium chain triglyceride) 5 times a week for 4 weeks. Urine was collected during the final 24 hours, and blood samples were centrifuged to obtain the serum.

All experiments were performed in accordance with Chugai Pharmaceutical Co.'s ethical guidelines for animal care, and the experimental protocols were approved by the animal care committee of the company and by the Animal Experimentation Ethics Committee of the National Center for Geriatrics and Gerontology.

Bone analysis. For bone analysis, right femurs and lumbar vertebrae were dissected and stored in 70% ethanol. BMD was measured by dual-energy x-ray absorptiometry (DCS-600EX; ALOKA Inc.). Left femurs and lumbar vertebrae were fixed in 4% paraformaldehyde for bone histomorphometry as described previously (7, 8). Each sample was sectioned, and then stained for tartrate-resistant acid phosphatase (TRAP). Histomorphometric parameters were measured at Niigata Bone Science Institute (Niigata, Japan).

Biochemical analysis. Serum and urinary calcium concentrations were determined using an autoanalyzer (Hitachi 7170). Urinary deoxypyridinoline was measured with a PYRILINKS-D assay kit (Metra Biosystems Inc.).

Osteoclastogenesis assay in vitro. Bone marrow cells were isolated from the tibiae and femurs of 6- to 9-week-old male C57BL/6J mice (SLC) and *VDR* KO mice (kindly provided by Shigeaki Kato, University of Tokyo, Tokyo, Japan). All cells were plated in culture dishes containing α-MEM/10% heat-inactivated FBS/1% antibiotics and incubated for 12 hours. Nonadherent cells were separated and cultured for 3 days with M-CSF (30 ng/ml), and then those that became adherent were used as osteoclast precursor cells. Cells were treated with RANKL (40 ng/ml) in the absence or presence of $1\alpha,25(OH)_2D_3$ for 3 days, fixed in 4% paraformaldehyde, and stained for TRAP. Multinucleate (≥3 nuclei), TRAP-positive cells were counted as osteoclasts. Osteoclast precursor cells were cultured in the presence of 30 ng/ml M-CSF without or with increasing doses of $1\alpha,25(OH)_2D_3$ for 3 days, and cell proliferation was assessed using a Cell Counting Kit-8 (Dojindo Laboratories).

Western and Northern analyses. Whole-cell extracts were isolated from osteoclast precursors, and protein concentrations were determined by use of a Bio-Rad Protein Assay kit (Bio-Rad Laboratories). Equivalent amounts of protein were loaded for 4–20% SDS-PAGE, and proteins transferred onto the membrane were detected with an ECL Plus Western blotting detection system (Amersham Biosciences). Phosphorylation of JNK, p38 MAPK, and IκB kinase was evaluated using kits from Cell Signaling Technology. Total RNA was isolated with TRIzol reagent (Invitrogen Corp.), according to the manufacturer's instructions. For Northern analysis, equal amounts of total RNA (10 μg/lane) were fractionated on a 1.5% agarose gel. The specific mRNAs were detected by hybridization of Hybond N^+ nylon membranes (Amersham Biosciences) with ^{32}P-labeled cDNA probes for mouse c-Fos, IFN-β, and NFATc1. For quantitative RT-PCR, total RNA (1 μg) was reverse transcribed using SuperScript III (Invitrogen Corp.), and samples were analyzed using a LightCycler (Roche Diagnostics Corp.). The primers included 5′-ACCTGTTCGTGAAACACACCA-3′ and 5′-ACAACACACTCCATGCGGTTT-3′ for c-Fos, 5′-GGACATTGGCATGATGAAGG-3′ and 5′-CTCAGACTGTCCTTCAAGGC-3′ for VDR, and 5′-TGCTGCCATTGTTGATATGG-3′ and 5′-TCCACAGCTTTGATGACACC-3′ for EF-1α. The amount of c-Fos and VDR mRNA was corrected by that of EF-1α mRNA.

Pulse-labeling and pulse-chase labeling experiments. For pulse labeling, osteoclast precursor cells were stimulated with RANKL for 24 hours in the absence or presence of $1\alpha,25(OH)_2D_3$ at 10^{-7} M and then radiolabeled for 1 hour with culture medium containing 150 μCi/ml of a ^{35}S-methionine and cysteine mixture (Amersham Biosciences). In the case of pulse-chase labeling, RANKL-treated osteoclast precursors were similarly radiolabeled and then incubated in the presence of nonradioactive medium containing 10 mM cold methionine and 10 mM cold cysteine for various periods of time. Cell extracts were immunoprecipitated with anti–c-Fos antibody, and the precipitates were then subjected to SDS-PAGE. After the gels had been dried, autoradiography was performed.

Retroviral expression of c-Fos protein. A retroviral vector encoding mouse c-Fos (pBabe-cFos, kindly provided by K. Matsuo, Keio University, Tokyo, Japan) was used to transfect Plat-E retrovirus packaging cells (a gift from T. Kitamura, University of Tokyo, Tokyo, Japan). The culture media were collected 48 hours after the transfection and kept as retrovirus stocks. Osteoclast precursor cells were exposed to the retrovirus in the presence of polybrene (8 μg/ml) for 1 day and were subsequently treated with RANKL and $1\alpha,25(OH)_2D_3$ for 4 days in the presence of puromycin (1.6 μg/ml). Osteoclast differentiation was evaluated as described above.

Statistics. Data were expressed as the means ± SEM. Statistical analysis was carried out by ANOVA, using Statistical Analysis System software (SAS Institute Inc.). The significance of differences was determined using 2-tailed Student's t test and Dunnett's multiple test. A value of $P < 0.05$ was considered to indicate a significant difference.

Acknowledgments

We thank Shigeaki Kato and Toshio Kitamura (University of Tokyo) for providing VDR KO mice and retroviral vectors, respectively; Koichi Matsuo, Sunao Takeshita, and Ken Watanabe (National Center for Geriatrics and Gerontology) for valuable suggestions; Mie Suzuki (National Center for Geriatrics and Gerontology) for expert technical assistance; and Akemi Ito (Niigata Bone Science Institute) for discussion on the data of bone histomorphometry. This study was supported in part by grants from the program Comparative Research on Aging and Health of the Ministry of Health, Labor, and Welfare of Japan (to K. Ikeda) and by a grant from the Program for Promotion of Fundamental Studies in Health Sciences of the National Institute of Biomedical Innovation of Japan (MF-14 to K. Ikeda).

Received for publication February 14, 2005, and accepted in revised form November 8, 2005.

Address correspondence to: Kyoji Ikeda, Department of Bone and Joint Disease, Research Institute, National Center for Geriatrics and Gerontology, 36-3 Gengo, Morioka, Obu, Aichi 474-8522, Japan. Phone and Fax: 81-562-46-8094; E-mail: kikeda@nils.go.jp.

1. Cummings, S.R., and Melton, L.J. 2002. Epidemiology and outcomes of osteoporotic fractures. *Lancet.* **359**:1761–1767.
2. Teitelbaum, S.L. 2000. Bone resorption by osteoclasts. *Science.* **289**:1504–1508.
3. Suda, T., et al. 1999. Modulation of osteoclast differentiation and function by the new members of the tumor necrosis factor receptor and ligand families. *Endocr. Rev.* **20**:345–357.
4. Karsenty, G., and Wagner, E.F. 2002. Reaching a genetic and molecular understanding of skeletal development. *Dev. Cell.* **2**:389–406.
5. Parfitt, A.M., et al. 1996. A new model for the regulation of bone resorption, with particular reference to the effects of bisphosphonates. *J. Bone Miner. Res.* **11**:150–159.
6. Rodan, G.A., and Martin, T.J. 2000. Therapeutic approaches to bone diseases. *Science.* **289**:1508–1514.
7. Shiraishi, A., et al. 2000. Alfacalcidol inhibits bone resorption and stimulates formation in an ovariectomized rat model of osteoporosis: distinct actions from estrogen. *J. Bone Miner. Res.* **15**:770–779.
8. Uchiyama, Y., et al. 2002. ED-71, a vitamin D analog, is a more potent inhibitor of bone resorption than alfacalcidol in an estrogen-deficient rat model of osteoporosis. *Bone.* **30**:582–588.
9. Shibata, T., et al. 2002. Vitamin D hormone inhibits osteoclastogenesis in vivo by decreasing the pool of osteoclast precursors in bone marrow. *J. Bone Miner. Res.* **17**:622–629.
10. Manolagas, S.C., and Jilka, R.L. 1995. Bone marrow, cytokines, and bone remodeling. Emerging insights into the pathophysiology of osteoporosis. *N. Engl. J. Med.* **332**:305–311.
11. Pacifici, R. 1996. Estrogen, cytokines, and pathogenesis of postmenopausal osteoporosis. *J. Bone Miner. Res.* **11**:1043–1051.
12. Shevde, N.K., Bendixen, A.C., Dienger, K.M., and Pike, J.W. 2000. Estrogens suppress RANK ligand-induced osteoclast differentiation via a stromal cell independent mechanism involving c-Jun repression. *Proc. Natl. Acad. Sci. U. S. A.* **97**:7829–7834.
13. Simonet, W.S., et al. 1997. Osteoprotegerin: a novel secreted protein involved in the regulation of bone density. *Cell.* **89**:309–319.
14. Bucay, N., et al. 1998. Osteoprotegerin-deficient mice develop early onset osteoporosis and arterial calcification. *Genes Dev.* **12**:1260–1268.
15. Reichel, H., Koeffler, H.P., and Norman, A.W. 1989. The role of the vitamin D endocrine system in health and disease. *N. Engl. J. Med.* **320**:980–991.
16. Ferrara, P., et al. 2003. The structural determinants responsible for c-Fos protein proteasomal degradation differ according to the conditions of expression. *Oncogene.* **22**:1461–1474.
17. Grigoriadis, A.E., et al. 1994. c-Fos: a key regulator of osteoclast-macrophage lineage determination and bone remodeling. *Science.* **266**:443–448.
18. Matsuo, K., et al. 2000. Fosl1 is a transcriptional target of c-Fos during osteoclast differentiation. *Nat. Genet.* **24**:184–187.
19. Takayanagi, H., et al. 2002. Induction and activation of the transcription factor NFATc1 (NFAT2) integrate RANKL signaling in terminal differentiation of osteoclasts. *Dev. Cell.* **3**:889–901.
20. Takayanagi, H., et al. 2002. RANKL maintains bone homeostasis through c-Fos-dependent induction of interferon-beta. *Nature.* **416**:744–749.
21. Matsuo, K., et al. 2004. Nuclear factor of activated T-cells (NFAT) rescues osteoclastogenesis in precursors lacking c-Fos. *J. Biol. Chem.* **279**:26475–26480.
22. Yoshizawa, T., et al. 1997. Mice lacking the vitamin D receptor exhibit impaired bone formation, uterine hypoplasia and growth retardation after weaning. *Nat. Genet.* **16**:391–396.
23. Thomas, M.K., et al. 1998. Hypovitaminosis D in medical inpatients. *N. Engl. J. Med.* **338**:777–783.
24. Trivedi, D.P., Doll, R., and Khaw, K.T. 2003. Effect of four monthly oral vitamin D3 (cholecalciferol) supplementation on fractures and mortality in men and women living in the community: randomised double blind controlled trial. *BMJ.* **326**:469–475.
25. Hauselmann, H.J., and Rizzoli, R. 2003. A comprehensive review of treatments for postmenopausal osteoporosis. *Osteoporos. Int.* **14**:2–12.
26. Papadimitropoulos, E., et al. 2002. Meta-analyses of therapies for postmenopausal osteoporosis. VIII. Meta-analysis of the efficacy of vitamin D treatment in preventing osteoporosis in postmenopausal women. *Endocr. Rev.* **23**:560–569.
27. Raisz, L.G., Trummel, C.L., Holick, M.F., and DeLuca, H.F. 1972. 1,25-Dihydroxycholecalciferol: a potent stimulator of bone resorption in tissue culture. *Science.* **175**:768–769.
28. Yasuda, H., et al. 1998. Osteoclast differentiation factor is a ligand for osteoprotegerin/osteoclastogenesis-inhibitory factor and is identical to TRANCE/RANKL. *Proc. Natl. Acad. Sci. U. S. A.* **95**:3597–3602.
29. Itonaga, I., Sabokbar, A., Neale, S.D., and Athanasou, N.A. 1999. 1,25-Dihydroxyvitamin D(3) and prostaglandin E(2) act directly on circulating human osteoclast precursors. *Biochem. Biophys. Res. Commun.* **264**:590–595.
30. Shiraishi, A., et al. 1999. The advantage of alfacalcidol over vitamin D in the treatment of osteoporosis. *Calcif. Tissue Int.* **65**:311–316.
31. Ueno, Y., et al. 2003. In vivo administration of 1,25-dihydroxyvitamin D3 suppresses the expression of RANKL mRNA in bone of thyroparathyroidectomized rats constantly infused with PTH. *J. Cell. Biochem.* **90**:267–277.
32. Matsumoto, T., et al. 2005. A new active vitamin D, ED-71, increases bone mass in osteoporotic patients under vitamin D supplementation: a randomized, double-blind, placebo-controlled clinical trial. *J. Clin. Endocrinol. Metab.* **90**:5031–5036.
33. Lips, P. 2001. Vitamin D deficiency and secondary hyperparathyroidism in the elderly: consequences for bone loss and fractures and therapeutic implications. *Endocr. Rev.* **22**:477–501.
34. Endo, K., et al. 2000. 1,25-Dihydroxyvitamin D3 as well as its analogue OCT lower blood calcium through inhibition of bone resorption in hypercalcemic rats with continuous parathyroid hormone-related peptide infusion. *J. Bone Miner. Res.* **15**:175–181.
35. Choi, S.J., et al. 1999. Identification of human asparaginyl endopeptidase (legumain) as an inhibitor of osteoclast formation and bone resorption. *J. Biol. Chem.* **274**:27747–27753.
36. Zhou, H., et al. 2001. A novel osteoblast-derived C-type lectin that inhibits osteoclast formation. *J. Biol. Chem.* **276**:14916–14923.
37. Schrader, M., Kahlen, J.P., and Carlberg, C. 1997. Functional characterization of a novel type of 1 alpha,25-dihydroxyvitamin D3 response element identified in the mouse c-fos promoter. *Biochem. Biophys. Res. Commun.* **230**:646–651.
38. Candeliere, G.A., Prud'homme, J., and St-Arnaud, R. 1991. Differential stimulation of fos and jun family members by calcitriol in osteoblastic cells. *Mol. Endocrinol.* **5**:1780–1788.
39. Shevde, N.K., et al. 2002. A potent analog of 1alpha,25-dihydroxyvitamin D3 selectively induces bone formation. *Proc. Natl. Acad. Sci. U. S. A.* **99**:13487–13491.
40. Peleg, S., Uskokovic, M., Ahene, A., Vickery, B., and Avnur, Z. 2002. Cellular and molecular events associated with the bone-protecting activity of the noncalcemic vitamin D analog Ro-26-9228 in osteopenic rats. *Endocrinology.* **143**:1625–1636.

The EMBO Journal (2006) 25, 554–564 | © 2006 European Molecular Biology Organization | All Rights Reserved 0261-4189/06
www.embojournal.org

THE EMBO JOURNAL

A novel ubiquitin-binding protein ZNF216 functioning in muscle atrophy

Akinori Hishiya[1,2], Shun-ichiro Iemura[3], Tohru Natsume[3], Shinichi Takayama[2], Kyoji Ikeda[1] and Ken Watanabe[1,*]

[1]Department of Bone & Joint Disease, National Center for Geriatrics & Gerontology (NCGG), Obu, Aichi, Japan, [2]Program of Molecular Chaperone Biology, Department of Radiology, Medical College of Georgia, Augusta, GA, USA and [3]Japan Biological Information Research Center (JBIRC), National Institute of Advanced Industrial Science & Technology (AIST), Tokyo, Japan

The ubiquitin–proteasome system (UPS) is critical for specific degradation of cellular proteins and plays a pivotal role on protein breakdown in muscle atrophy. Here, we show that ZNF216 directly binds polyubiquitin chains through its N-terminal A20-type zinc-finger domain and associates with the 26S proteasome. ZNF216 was colocalized with the aggresome, which contains ubiquitinylated proteins and other UPS components. Expression of *Znf216* was increased in both denervation- and fasting-induced muscle atrophy and upregulated by expression of constitutively active FOXO, a master regulator of muscle atrophy. Mice deficient in *Znf216* exhibited resistance to denervation-induced atrophy, and ubiquitinylated proteins markedly accumulated in neurectomized muscle compared to wild-type mice. These data suggest that ZNF216 functions in protein degradation via the UPS and plays a crucial role in muscle atrophy.

The EMBO Journal (2006) **25,** 554–564. doi:10.1038/sj.emboj.7600945; Published online 19 January 2006
Subject Categories: proteins; molecular biology of disease
Keywords: aggresome; muscular atrophy; proteasome; ubiquitin; zinc-finger protein

Introduction

The ubiquitin–proteasome system (UPS) is one of the major protein degradation pathways in eukaryotic cells. The UPS plays key regulatory roles in many cellular processes, including cell cycle control, the regulation of transcription and protein quality control (Hershko and Ciechanover, 1998; Pickart and Cohen, 2004). Aberrations of this system lead to many forms of pathogenesis, such as malignancies, neurodegenerative disease and inflammatory response (Glickman and Ciechanover, 2002). The UPS includes sequential, multistep reactions: ubiquitin-conjugation of target proteins by E1, E2 and E3 enzymes, recognition of ubiquitinylated proteins by ubiquitin-binding proteins or 19S subunits of proteasome and proteolysis in the proteasome.

Many catabolic conditions, such as low-insulin state, hyperthyroidism, sepsis and cancer cachexia lead to enhancement of protein breakdown in skeletal muscle known as muscle atrophy (Mitch and Goldberg, 1996; Lecker *et al*, 1999). In muscle atrophy, the UPS plays a pivotal role in protein breakdown (Price *et al*, 1996; Tawa *et al*, 1997). Several studies indicate that mRNAs encoding UPS components are increased in atrophying muscle (Medina *et al*, 1991; Wing and Goldberg, 1993; Bailey *et al*, 1996; Price *et al*, 1996; Jagoe *et al*, 2002). In particular, the E3 ubiquitin ligases MAFbx/Atrogin-1 and MuRF-1 (muscle RING finger 1) are known to be markers of muscle atrophy (Bodine *et al*, 2001; Gomes *et al*, 2001). Both are induced in multiple models of muscle atrophy including immobilization, denervation and hindlimb suspension, and mice deficient in either gene are resistant to denervation-induced muscle atrophy (Bodine *et al*, 2001). Goldberg and co-workers proposed that atrophy-related genes, whose expression is induced in multiple types of muscle atrophy, are called 'atrogenes' (Sandri *et al*, 2004). Recently, it was demonstrated that the IGF-I/PI3K/Akt pathway is an important regulator of muscle mass in muscle hypertrophy and atrophy (Sacheck *et al*, 2004; Sandri *et al*, 2004; Stitt *et al*, 2004). In that case, the transcription factor FOXO plays a pivotal role in activating atrogenes such as MAFbx/Atrogin-1 (Gomes *et al*, 2001).

Although many UPS players such as E3 ligases have been characterized, the mechanism of how ubiquitinylated proteins are delivered to the proteasome have not been fully elucidated. A component of 19S proteasome, Rpn10/S5a, recognizes the ubiquitinylated proteins (Young *et al*, 1998; Wilkinson *et al*, 2000). It has been shown that yeast proteins, Rad23p and Dsk2p, bind to ubiquitinylated substrates and to the 26S proteasome through their UBA and Ubl domains, respectively, thereby functioning as shuttle proteins that present polyubiquitinylated proteins to the proteasome (Chen *et al*, 2001; Funakoshi *et al*, 2002; Elsasser and Finley, 2005). Loss-of-function of shuttle proteins results in abnormal accumulation of polyubiquitinylated proteins (Lambertson *et al*, 1999; Saeki *et al*, 2002). However, yeast can survive when both *RAD23* and *DSK2* genes are mutated, suggesting that other mechanisms or molecule(s) possessing a shuttle function exist (Saeki *et al*, 2002). Here, we show that ZNF216, a novel ubiquitin-binding protein containing an A20-type zinc-finger, is such a factor. *Znf216* expression is upregulated in skeletal muscle in experimental models of muscle atrophy, and *Znf216*-deficient mice exhibit resistance to muscle atrophy accompanied by abnormal accumulation of polyubiquitinylated proteins in skeletal muscle. Our findings suggest that ZNF216, with its potential function of anchoring ubiquitinylated proteins to the proteasome, plays a critical role in degrading muscle proteins.

*Corresponding author. Department of Bone & Joint Disease, National Center for Geriatrics & Gerontology (NCGG), Obu, Aichi 474-8522, Japan. Tel.: +81 562 46 2311; Fax: +81 562 44 6595;
E-mail: kwatanab@nils.go.jp

Received: 6 June 2005; accepted: 14 December 2005; published online: 19 January 2006

Results

ZNF216 directly binds to polyubiquitin

We have identified a gene, *Znf216* (*Za20d2*, Mouse Genome Informatics), encoding an A20 zinc-finger (Znf-A20) motif-containing protein, as a RANKL-induced gene upregulated upon osteoclast formation using a microarray technique (Hishiya *et al*, 2005). *Znf216* was originally identified as a candidate gene for hearing loss and is expressed in cochlear and skeletal muscle (Scott *et al*, 1998; Huang *et al*, 2004). To determine the function of ZNF216, we searched for molecules that associate with ZNF216 using yeast two-hybrid screening and isolated several clones encoding a gene for polyubiquitin C. To determine whether ZNF216 interacts with ubiquitin in mammalian cells, we transfected HEK293 cells with an expression vector for FLAG-tagged ZNF216 and HA-tagged ubiquitin and performed co-immunoprecipitation experiments. ZNF216 possesses A20-type (amino acids 11–35) and AN1-type (amino acids 154–191) zinc-finger domains at its N- and C-termini, respectively (Figure 1A). Endogenous ubiquitinylated proteins, which appear as smears, were co-immunoprecipitated with FLAG-tagged ZNF216 (Figure 1B). Notably, N-terminal deletion (ΔN; amino acids 36–213) or point mutants (M1 and M3) of the A20-type zinc-finger (ZnF-A20) domain abolished ubiquitin-binding ability of ZNF216, indicating that the ZnF-A20 domain is indispensable for binding to ubiquitin (Figures 1A and B). Whereas in non-denaturing conditions, ubiquitinylated molecules were present with FLAG-tagged ZNF216, these molecules completely disappear from immunoprecipitates following heat denaturation, which abolishes noncovalent protein–protein interactions (Figure 1C), suggesting that ZNF216 associates with ubiquitinylated proteins rather than being ubiquitinylated itself. Next, to determine whether ZNF216 binds to ubiquitin directly, we performed GST pull-down assays using GST-ZNF216 fusion proteins (Figure 1D) and purified polyubiquitin. As shown in Figure 1E, GST-ZNF216 but not GST bound to polyubiquitin chains. As expected, binding of ZNF216 to polyubiquitin chains was completely abolished by a point mutation in the ZnF-A20 domain (M1, Figure 1E). Furthermore, a GST fusion protein containing only the ZnF-A20 domain (amino acids 2–60) could bind to polyubiquitin chains, suggesting that ZNF216 directly binds to polyubiquitin chains, and that the ZnF-A20 domain is required for binding to polyubiquitin. As for other ZnF-A20 containing proteins, AWP1 (ZA20D3) also possessed polyubiquitin-binding activity but the ZnF-A20 domain(s) of Rabex-5 (Horiuchi *et al*, 1997) and A20/TNFAIP3 (Opipari *et al*, 1990) proteins did not (Supplementary Figure S1).

ZNF216 associates with the 26S proteasome

We also identified molecules associating with ZNF216 by proteomic analysis of complexes formed with FLAG-tagged ZNF216. Molecules expressed in HEK293 cells and that co-immunoprecipitated with FLAG-tagged ZNF216 were analyzed by tandem mass spectrometry. By this analysis, every subunit of the 26S proteasome complex was identified as associating with FLAG-tagged ZNF216 (data not shown). To identify the region of ZNF216 required for association with the 26S proteasome, lysates of cells expressing either FLAG-tagged ZNF216 or its mutants were immunoprecipitated with anti-FLAG antibody. Co-precipitation of proteasomal components was monitored by immunoblotting using an antibody against Rpn7p (S10a), a non-ATPase subunit of the 19S regulatory subunit. As shown in Figure 2A, this protein efficiently co-precipitated with FLAG-tagged ZNF216. The interaction was also observed with truncated or point mutants of ZnF-A20 (ΔN or M1), indicating that ubiquitin-binding ability is dispensable for association with the 26S proteasome. To determine whether endogenous ZNF216 proteins are also associated with the 26S proteasome, we performed a GST pull-down assay using the ubiquitin-like (Ubl) domain of hHR23B, a human homologue of Rad23, which is known to bind to the 26S proteasome. As shown in Figure 2B, GST-Ubl but not GST was pulled down with the endogenous 26S proteasome. Endogenous ZNF216 was also detected in the GST-Ubl/26S proteasome complex (upper panels, Figure 2B). Furthermore, purified recombinant ZNF216 did not bind to GST-Ubl (lower panel, Figure 2B), suggesting that endogenous ZNF216 is not directly bound to the Ubl domain but associates with the 26S proteasome.

Colocalization with the aggresome

Next, we determined the subcellular localization of ZNF216. Indirect immunofluorescence of ZNF216 expressed in COS-7 cells showed that the protein was largely cytoplasmic but was seen to a lesser extent in the nucleus (Figure 3A). Aggresomes, which are insoluble aggregates of ubiquitinylated proteins complexed with the proteasome and induced by treatment with proteasome inhibitors, are known to mimic inclusions seen in pathogenic UPS disorders (Johnston *et al*, 1998; Kopito, 2000; Lelouard *et al*, 2002). As shown in Figures 3D–H, ZNF216 proteins were colocalized with aggresomes induced by treatment with the proteasome inhibitor MG132. ZNF216 itself was not ubiquitinylated as shown in Figure 1C.

Induction of ZNF216 expression upon muscle atrophy

Biochemical and cell biological evidence presented here strongly suggests that ZNF216 functions in the UPS. In skeletal muscle, it is generally accepted that the UPS plays a critical role in muscular atrophy, and expression of atrophy-related genes including those encoding UPS components is induced in atrophying muscle (Jagoe *et al*, 2002; Lecker *et al*, 2004). As *Znf216* was predominantly expressed in brain and skeletal muscle (Scott *et al*, 1998), we investigated the relationship between ZNF216 and muscle atrophy. To determine whether *Znf216* expression is induced during muscle atrophy, an *in vitro* model of muscle atrophy was utilized. It has been reported that addition of dexamethasone to cultures of differentiated C2C12 myotubes causes formation of myotubes exhibiting signs of atrophy, including a reduction in myotube diameter (Stitt *et al*, 2004). Such treatment dramatically induced expression of *Znf216* (Figure 4A).

Next, expression of *Znf216* was determined in *in vivo* experimental models of muscle atrophy. Mice that undergo fasting for 2 days show significant decreases in body weight, as well as in the mass of the gastrocnemius muscles (data not shown). In this model, fasting for 2 days results in dramatic increases in *Znf216* mRNA (Figure 4B) and protein (Supplementary Figure S3) in muscle. Although there were differences in induction patterns of two differently sized transcripts of Znf216 by atrophy-inducting stimuli, both transcripts encode the same protein (Supplementary Figures

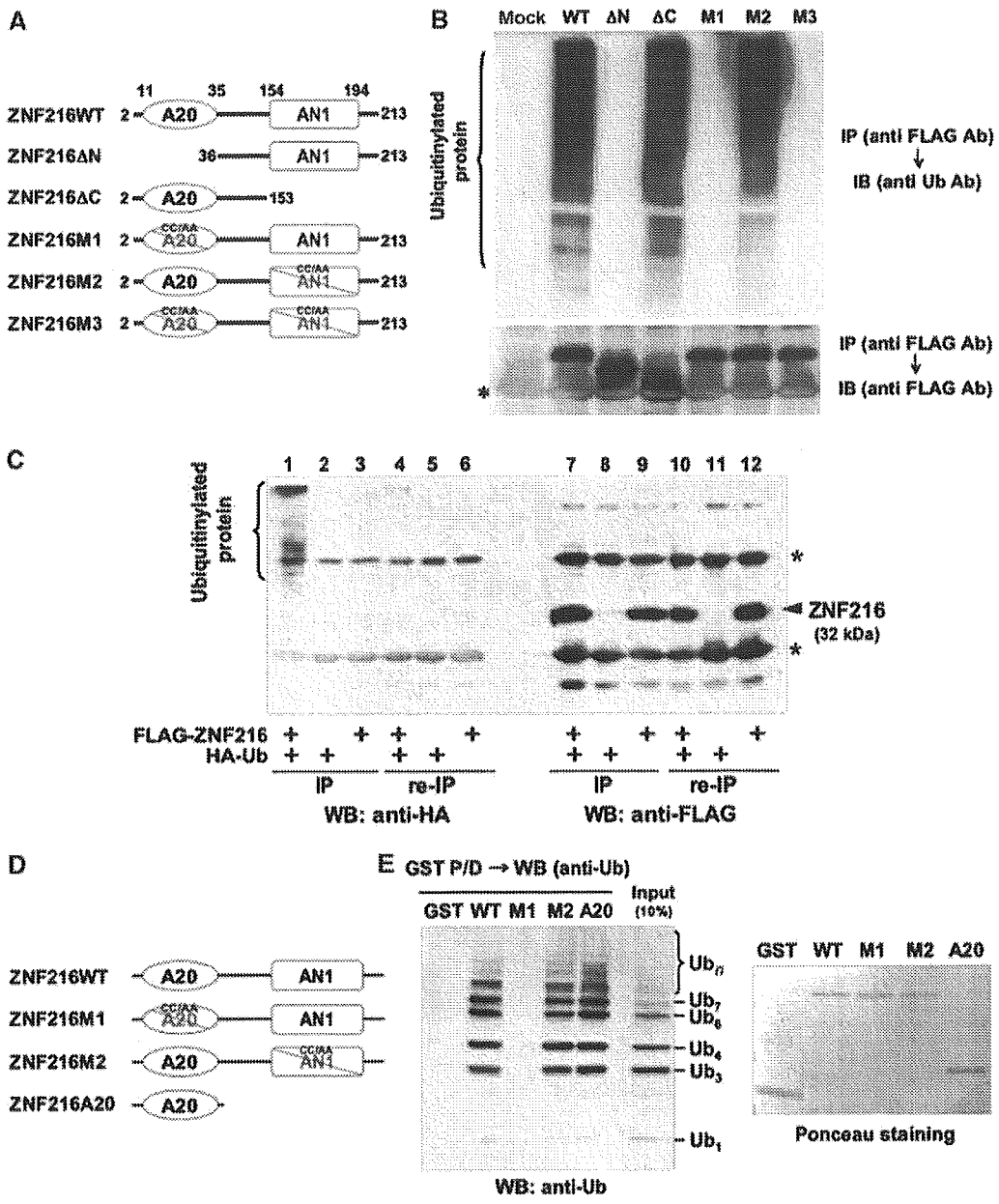

Figure 1 ZNF216 binds polyubiquitin directly through the ZnF-A20 domain. (**A**) Schematic representation of the primary structure of wild-type ZNF216 and its mutants. ZNF216ΔN (aa 36–213) and ZNF216ΔC (aa 2–153) constructs lack the ZnF-A20 (aa 11–35) and ZnF-AN1 (aa 154–194) domains, respectively. Cysteine residues at positions 30 and 33 within the ZnF-A20 were substituted with alanines (C30A/C33A) in ZNF216M1, and both cysteines 170 and 175 within the ZnF-AN1 were substituted with alanines (C170A/C175A) in ZNF216M2. Both ZnF-A20 and ZnF-AN1 domains were mutated in ZNF216M3. (**B**) Co-precipitation of ubiquitinylated proteins and ZNF216. FLAG-tagged ZNF216 or mutants were expressed in HEK293 cells, and cell extracts were immunoprecipitated with anti-FLAG antibody. Ubiquitinylated proteins detected with anti-ubiquitin antibody were precipitated with FLAG-tagged ZNF216 but not with ZnF-A20 mutants. Expression levels of FLAG-tagged ZNF216 constructs are shown at the bottom. Bands corresponding to immunoglobulin chains are marked by an asterisk. (**C**) ZNF216 is minimally ubiquitinylated. HEK293 cells expressing FLAG-tagged ZNF216 or HA-tagged ubiquitin were lysed and immunoprecipitation was performed using anti-FLAG antibody. Aliquots of precipitated beads were boiled and immunoprecipitated again (re-IP). Each sample was separated on gels and probed with anti-HA (left) or anti-FLAG antibody (right). Bands for immunoglobulin chains are marked by asterisks. (**D**) Constructs used for *in vitro* binding assay. ZNF216WT, ZNF216M1 and ZNF216 M2 were as indicated in (A). ZNF216A20 possesses only the A20 domain (aa 2–60). All constructs were produced as GST fusion proteins. (**E**) *In vitro* ubiquitin binding assay. Left panel: GST protein fused to the constructs indicated in (D) was incubated with purified K48-linked polyubiquitin chains, followed by precipitation with GSH beads. In all, 10% of purified polyubiquitin chains was separated without pull-down to evaluate protein amount (10% input). Right panel: the membrane was stained with ponceau to evaluate levels of GST fusion protein.

S2 and S3). Expression of MuRF-1 (Figure 4B) and MAFbx (Gomes *et al*, 2001) was also induced in fasting. Upregulation of *Znf216* was also observed in a model of denervation-induced muscle atrophy. Neurectomy promotes significant reduction (~20%) in the weight of gastrocnemius muscles within the first 7 days postsurgery. As expected, expression of *Znf216* and MuRF-1 was induced in gastrocnemius muscles by denervation-induced muscle atrophy (Figure 4C). These results suggest that *Znf216* expression is associated with atrophy in skeletal muscles.

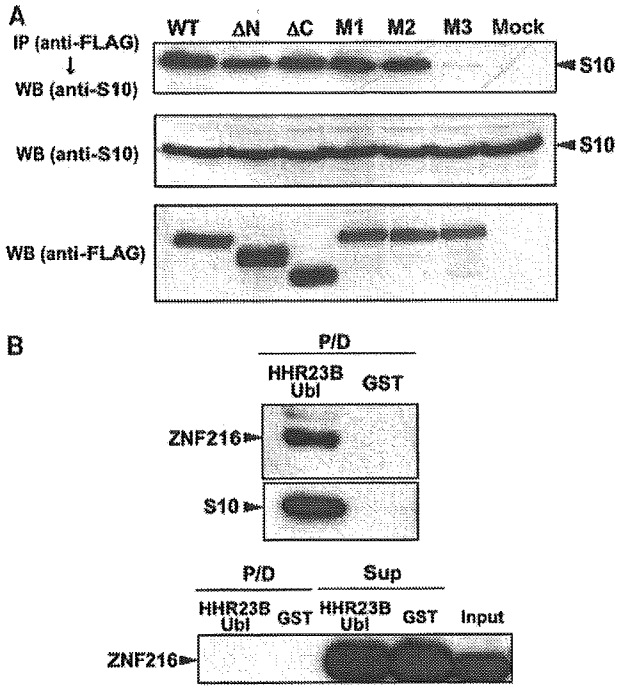

Figure 2 Interaction of ZNF216 with the 26S proteasome in mammalian cells. (**A**) Co-precipitation of the 26S proteasome and ZNF216. Co-precipitated proteins with FLAG-ZNF216 were resolved by SDS–PAGE and detected by immunoblotting using anti-S10a/Rpn7p antibody (anti-S10) or anti-FLAG antibody. Aliquots of cellular extracts were immunoblotted without immunoprecipitation to evaluate protein expression in the bottom panels. (**B**) ZNF216 was detected in the 26S proteasome fraction. Upper panel, cell lysates were incubated with a GST fusion of HHR23B Ubl (HHR23B Ubl) to isolate the 26S proteasome. Precipitated proteins (P/D) were separated and probed with anti-S10 or anti-ZNF216 antibody. Lower panel: purified recombinant ZNF216 was incubated with a GST fusion of HHR23B Ubl or GST protein. Precipitated (P/D) or not precipitated (Sup) proteins were probed with anti-ZNF216 antibody. No direct binding of ZNF216 to the Ubl domain of HHR23B was detected.

The transcription factor FOXO has been reported to play a critical role in muscular atrophy by inducing atrophy-related genes, including MAFbx/Atrogin-1 (Sandri *et al*, 2004; Stitt *et al*, 2004). Therefore, we asked whether FOXO activation upregulated *Znf216* expression. To do so, we employed a Cre-loxP system (Furukawa-Hibi *et al*, 2002) in which constitutively active FOXO4 (AFX-TM) created by mutation of the three Akt phosphorylation sites, T32A, S253A and S315A (Brunet *et al*, 1999), was expressed in C2C12-AFX-TM cells following infection by Cre recombinase-expressing adenovirus (Cre) (Figure 4D). Both AFX-TM mRNA and protein were induced 24 h after infection with Cre but not with control adenovirus (Furukawa-Hibi *et al*, 2002). ZNF216 mRNA was markedly increased in C2C12-AFX-TM cells as a result of infection with Cre but not following infection with control virus (Figure 4E). These results suggest that ZNF216 may function as a downstream effector of FOXO in muscle atrophy.

Generation of mice lacking ZNF216

To investigate the *in vivo* function of ZNF216, mice deficient for ZNF216 ($Znf216^{lex/lex}$) were generated by gene trapping at Omnibank of Lexicon Genetics (Zambrowicz *et al*, 1998). The structure of the predicted trapped gene is shown in Figure 5A. The trapping vector, VICTR48, was inserted 3.3 kbp upstream of exon 3, which encodes the first methionine of mouse *Znf216* (Figure 5A). $Znf216^{lex/lex}$ mice were born from interbred heterozygous $Znf216^{+/lex}$ mice in Mendelian ratios, indicating that ZNF216 is dispensable for embryogenesis or fetal development. No ZNF216 mRNA or protein was detected in $Znf216^{lex/lex}$ mice by Northern or immunoblot analyses, respectively (Figures 5B and C), indicating that the mice are ZNF216 nulls. Expression levels of ZNF216 in $Znf216^{+/lex}$ heterozygotes were nearly one-half those of wild-type mice. $Znf216^{lex/lex}$ mice were viable and fertile, without gross abnormalities or apparent pathological alteration, but they weighed less than sex- and age-matched controls (Figure 5D). At 45 weeks, the average weights of $Znf216^{+/+}$ and

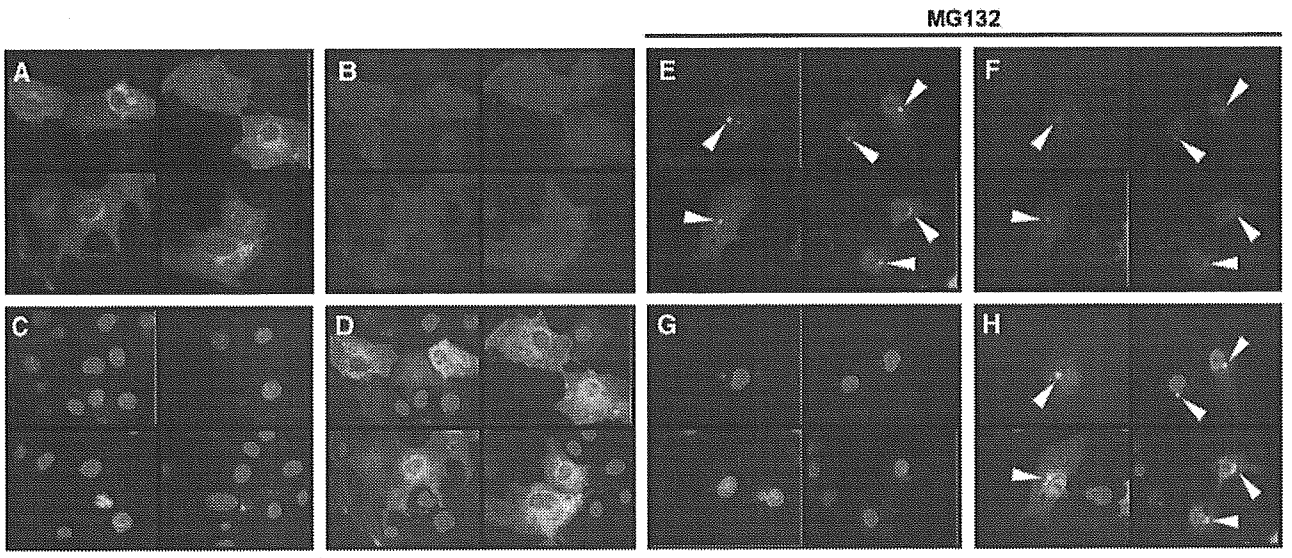

Figure 3 ZNF216 is localized in 'aggresomes' with ubiquitinylated proteins. (**A–H**) COS cells were transfected with expression vectors for FLAG-tagged ZNF216 and HA-tagged ubiquitin. Fixed cells were subjected to indirect immunofluorescence using (A, E) anti-FLAG (with AlexaFluor 488 anti-mouse IgG, green) and (B, F) anti-HA (with AlexaFluor 546 anti-rat IgG antibodies, red) antibodies. (C, G) Nuclei were stained with DAPI in the same fields of each panel. (E–H) Transfected COS cells were treated with the proteasome inhibitor, MG132 (0.5 μM). Aggresomes formed are indicated by arrowheads. The merged images were shown in (D and H).

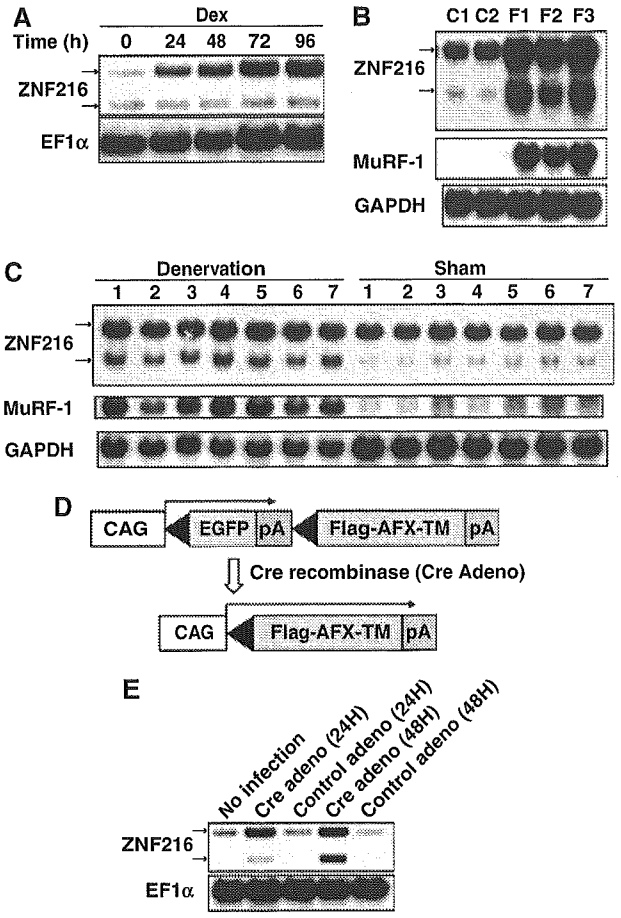

Figure 4 Expression of ZNF216 is induced by muscle atrophy. (**A**) C2C12 myoblast cells were differentiated into myotubes, and treated with 100 μM Dex for the indicated times. Northern blotting was performed to reveal the effect of Dex on ZNF216 expression. The entire coding region of ZNF216 was used as a probe, which recognized 2.4 and 1.5 kb mRNA species arising from alternative splicing and polyadenylation. The loading control was elongation factor α (EF1α). (**B**) Fasting-induced muscle atrophy. Three mice were fasted (F1 ~ F3), and two mice (C1, C2) were fed freely. After 2 days, RNA was purified from gastrocnemius muscle, and Northern blotting was performed to determine ZNF216 expression. The membrane was re-probed with MuRF-1 and GAPDH. (**C**) Denervation-induced muscle atrophy was induced by cutting the sciatic nerve of the hindlimb of seven mice (1 ~ 7). The opposite limb was sham operated as the control. At 7 days after surgery, total RNA was purified from gastrocnemius muscles, and Northern blotting was performed to detect ZNF216 expression. The membrane was re-probed with MuRF-1 and GAPDH. (**D**) Cre-loxP-mediated, constitutively active FOXO expression system. cDNA encoding FLAG-tagged constitutively active FOXO4 (AFX-TM) is separated from the CAG promoter of an expression vector by a loxP-flanked EGFP-poly(A) cassette. Infection with adenovirus expressing Cre recombinase (Cre) results in excision of the DNA fragment located between the two loxP sequences and expression of FLAG-tagged AFX-TM. (**E**) ZNF216 is downstream of FOXO. Total RNAs were prepared from C2C12-AFX-TM cells at the indicated times after infection with adenovirus expressing Cre (Cre) or lacZ (control) and probed by *Znf216* or EF1α. A marked increase in expression of *Znf216* was observed only in Cre-infected cells.

Znf216$^{lex/lex}$ male mice were 42.66 ± 7.06 g ($n = 14$) and 33.16 ± 4.44 g ($n = 9$), respectively. The average weights of female *Znf216*$^{+/+}$ and *Znf216*$^{lex/lex}$ mice were 34.46 ± 4.21 g ($n = 14$) and 26.85 ± 5.38 g ($n = 11$), respectively. After 30 weeks, both female and male *Znf216*$^{lex/lex}$ mice showed no or subtle increases in weight, whereas *Znf216*$^{+/+}$ or

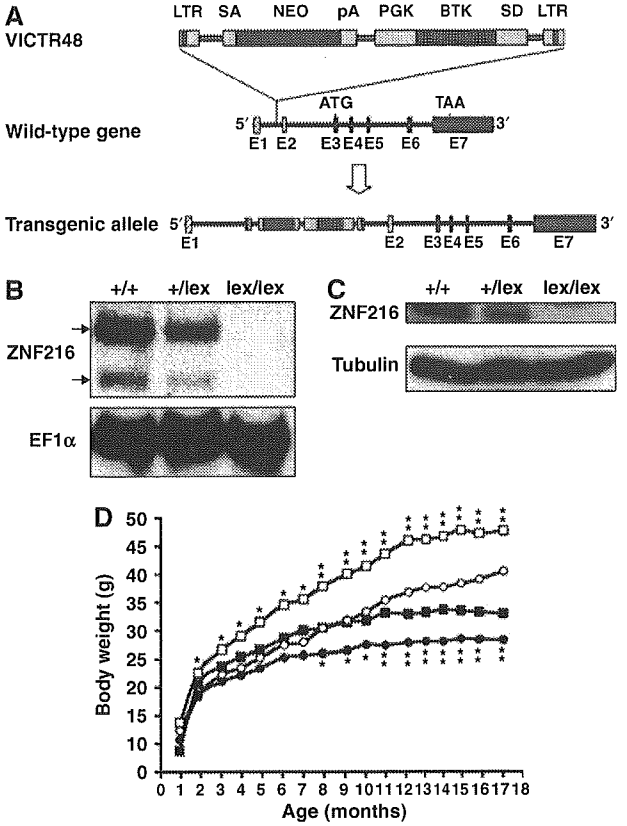

Figure 5 Disruption of *Znf216* gene in mice. (**A**) Gene trap strategy of *Znf216* gene. The structure of the trapping vector, VICTR48, is shown in the upper line. The wild-type allele and the trapped, transgenic allele follow the vector. The retroviral vector, VICTR48, was integrated between exons 1 and 2 of the *Znf216* gene and transcription of downstream exons encoding ZNF216 was diminished. Exons are depicted by striped (noncoding exons) or shadowed boxes (protein-coding exons) and numbered (E1 and E2). LTR, long terminal repeat; SA, splice acceptor site; SD, splice donor site; pA, polyadenylation signal; PGK, PGK promoter. (**B**) Northern blot analysis. Total RNA was prepared from brains of *Znf216*$^{+/+}$, *ZnfF216*$^{+/lex}$ or *Znf216*$^{lex/lex}$ mice. Full-length mouse ZNF216 cDNA was used as a probe. The membrane was re-probed using an EF1α probe. (**C**) Immunoblot analysis. Extracts from brain of *Znf216*$^{+/+}$, *Znf216*$^{+/lex}$ or *Znf216*$^{lex/lex}$ mice were immunoblotted with antibody against ZNF216. The membrane was re-probed using anti-tubulin antibody. (**D**) Growth curve of *Znf216*$^{lex/lex}$ mice. Body weights at each time point of *Znf216*$^{+/+}$ and *Znf216*$^{lex/lex}$ mice were indicated as open square boxes (males) or circles (females) and closed square boxes (males) or circles (females), respectively. $^{*}P < 0.05$; $^{**}P < 0.005$.

Znf216$^{+/lex}$ mice gained weight as they aged (Figure 5D). The size of most organs in *Znf216*$^{lex/lex}$ mice was reduced in proportion with body weight. However, the fat volume of aged (> 30 weeks of age) *Znf216*$^{lex/lex}$ mice was significantly decreased, suggesting that the marked difference in body weight between wild-type and aged *Znf216*$^{lex/lex}$ mice is mainly caused by decreased fat mass seen in *Znf216*$^{lex/lex}$ mice (not shown). Detailed phenotypic characterization of aged mutant mice will be provided elsewhere.

Znf216$^{lex/lex}$ mice exhibit partial resistance to denervation-induced muscle atrophy

To further explore the involvement of ZNF216 in muscle atrophy, neurectomy of sciatic nerve was undertaken in wild-type and *Znf216*$^{lex/lex}$ mice. As shown in Figure 6A, 7

days after denervation, significant muscle weight loss and reduction in fiber sizes of the gastrocnemius muscle were observed in wild-type mice. By contrast, such decreases in muscle weight were significantly attenuated in *Znf216*$^{lex/lex}$ mice (Figure 6A). Sections of gastrocnemius muscle also showed larger fibers in muscle from neurectomized *Znf216*$^{lex/lex}$ mice than in control muscle (Figure 6B). However, there was no significant difference in fiber area between sham-operated wild-type and *Znf216*$^{lex/lex}$ mice (wild type + sham operated, $1988 \pm 530\,\mu m^2$; wild type + denervation, $1379 \pm 345\,\mu m^2$; lex/lex + sham operated, $1776 \pm 484\,\mu m^2$; lex/lex + denervation, $1393 \pm 344\,\mu m^2$). As shown in Figure 6C, the reduction in fiber area was also less apparent in *Znf216*$^{lex/lex}$ mice compared to wild-type mice. These results suggest that ZNF216 plays a crucial role in reduction of muscle mass on denervation-induced muscle atrophy.

Abnormal accumulation of ubiquitinylated proteins in muscle from Znf216$^{lex/lex}$ *mice*

To investigate what abnormalities occur during denervation-induced muscle atrophy in *Znf216*$^{lex/lex}$ mice, we examined

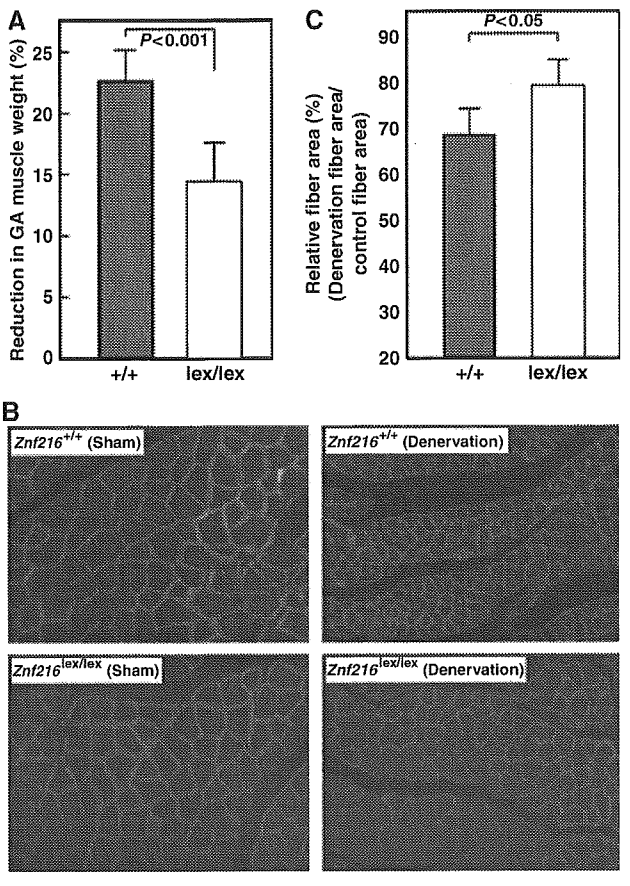

Figure 6 Denervation induced muscular atrophy was attenuated in *ZNF216*$^{lex/lex}$ mice. (**A**) Reduction of GA muscle weight upon neurectomy. Percent decreases in muscle weights are shown as a percent of control, calculated as the left/right muscle weights. (**B**) Cross-sections from gastrocnemius muscle were stained by indirect immunofluorescence with anti-laminin. The reduction in size was also significant in muscle fibers of control mice but less in *Znf216*$^{lex/lex}$. (**C**) Muscle fiber cross-sectional areas were measured in transverse tissue section (B). Percent relative fiber area of denervated muscle to control fiber area (sham-operated) are shown.

expression levels of factors involved in muscle atrophy. As expected, expression of MAFbx/Atrogin-1 and MuRF-1 was dramatically induced by denervation-induced muscle atrophy in gastrocnemius muscle from wild-type mice (Figure 6A). In *Znf216*$^{lex/lex}$ mice, expression of MAFbx/Atrogin-1 and MuRF-1 was also induced at levels comparable to those seen in wild-type mice. Induction of *Pmsa1* and *Pmsd11*, genes encoding the 26S proteasome subunits α6 and Rpn6, respectively, was also indistinguishable between *Znf216*$^{lex/lex}$ and wild-type mice (Figure 7A). Furthermore, proteasome activities in gastrocnemius muscles were comparable between wild-type and *Znf216*$^{lex/lex}$ mice (Figure 7B). Thus, induction of relevant ubiquitin ligases or proteasome components was not affected in *Znf216*$^{lex/lex}$ mice. It is known that ubiquitinylated proteins accumulate during muscle atrophy (Medina *et al*, 1991; Wing *et al*, 1995). As shown in Figure 7C, following denervation, ubiquitinylated proteins accumulated in the gastrocnemius muscle of wild-type mice, but higher levels of ubiquitinylated proteins accumulated in muscle derived from *Znf216*$^{lex/lex}$ mice (~2-fold: $P<0.001$ in neurectomized *Znf216*$^{lex/lex}$ versus wild-type muscle). Similar results were obtained by fasting-induced muscle atrophy, although no difference in the levels of ubiquitinylated proteins from controls (sham-operated or fed) was observed between genotypes (Figure 7C). These results indicate that ZNF216 is a critical regulator of muscle atrophy, most likely functioning to regulate degradation of muscle proteins without altering expression of proteasomal components or known E3 ligases.

Effect of ZNF216 on UPS-mediated protein degradation

Accumulation of ubiquitinylated protein under any circumstance might be because of loss of inhibition of ubiquitinylation and/or deubiquitinylation (DUB). However, no inhibition or DUB activity was observed (Supplementary Figures S4 and S5). As shown in Figure 7D, association of ZNF216 protein to the proteasome was significantly increased when atrophy was induced, suggesting that ZNF216 may be involved in association of ubiquitinylated proteins and the proteasome. The biochemical activity of ZNF216 is similar to that of the UPS proteins, hHR23 and hPLIC, both of which have a shuttle function and are known to bind to both polyubiquitinylated proteins and the 26S proteasome (Hartmann-Petersen and Gordon, 2004; Elsasser and Finley, 2005). Interestingly, overexpression of hHR23 and hPLIC results in stabilization of unstable proteins such as p53 (Kleijnen *et al*, 2000; Glockzin *et al*, 2003). To determine if ZNF216 functioned similarly, we employed a degradation system using unstable GFP (Bence *et al*, 2001). In this system, the CL1 peptide, which functions as a degron, is fused to EGFP (EGFP-CL1). Degradation by conjugation with the degron is mediated by the UPS (Bence *et al*, 2001). EGFP-CL1, constitutively expressed in HEK293 cells, is unstable and the estimated half-life ($t_{1/2}$) of EGFP-CL1 in this system is about 11 min. Ubiquitinylated EGFP-CL1 protein stabilized by treatment with a proteasome inhibitor was associated with ZNF216 but EGFP itself was not (not shown). As shown in Figure 8A, protein degradation was markedly retarded in the presence of ectopic ZNF216 ($t_{1/2}>30$ min) compared to cells transfected with the loss of function mutant ZNF216M3 or mock-transfected cells. Rapid turnover of EGFP-CL1 protein was inhibited by treatment with the

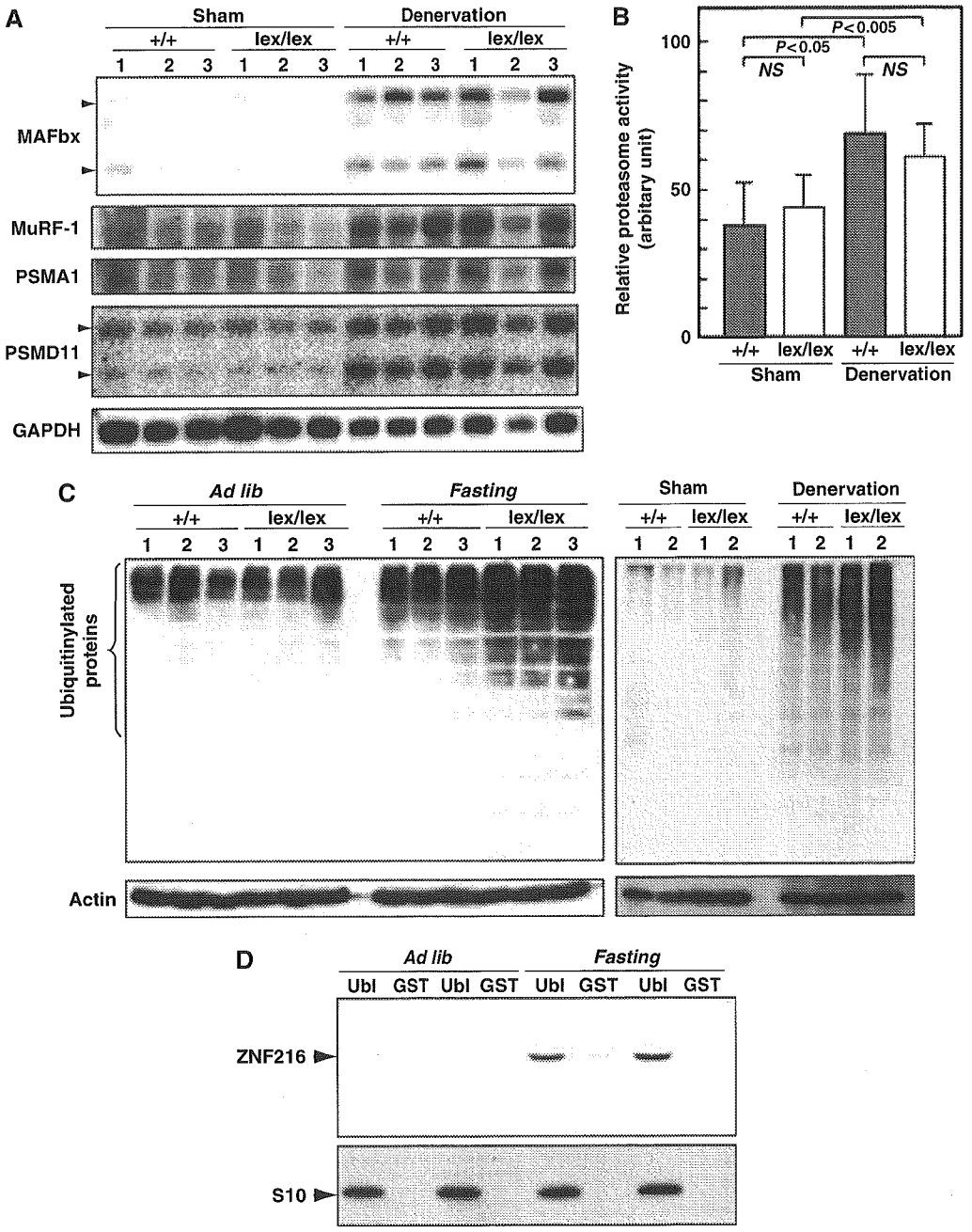

Figure 7 Changes in UPS upon muscular atrophy. (**A**) Expression of UPS components in denervation-induced muscular atrophy. Total RNAs were purified from gastrocnemius muscle, and Northern blotting was performed using indicated probes. Expression of genes for ubiquitin-ligases, such as MAFbx or MuRF-1, and proteasome subunits PSMA1 and PSMD11 was induced by muscle atrophy at comparable levels between wild-type and *ZNF216*$^{lex/lex}$ mice. (**B**) Proteasome activity. Proteasome activities in muscle extracts from wild-type or *ZNF216*$^{lex/lex}$ mice were measured and are shown as arbitrary units. No significant difference in proteasome activity between wild-type and *ZNF216*$^{lex/lex}$ was observed. (**C**) High levels of ubiquitinylated proteins accumulated in muscles from *ZNF216*$^{lex/lex}$ mice than in muscles from wild-type mice. Muscle extracts from wild-type or *ZNF216*$^{lex/lex}$ mice were subjected to immunoblotting using anti-ubiquitin antibody to analyze levels of ubiquitinylated proteins. Left and right panels show fasting-induced and denervation-induced muscle atrophy, respectively. Each membrane was re-probed with anti-actin antibody. (**D**) Association of ZNF216 with the proteasome was increased upon atrophy. The proteasome fractions in muscle extracts from fed (*ad lib*) or fasted (fasting) mice were precipitated with GST-Ubl or GST only as a negative control. Endogenous ZNF216 protein was co-precipitated with the proteasome, which is probed by the anti-S10 antibody.

proteasome inhibitor MG132 (MG132, Figure 8B). The levels of the proteins stabilized by MG132 were comparable among cells transfected with ZNF216 constructs, indicating that protein synthesis of EGFP-CL1 was not significantly affected by ectopic expression of ZNF216 (MG132, Figure 8B). ZNF216WT, and to a lesser extent the mutants M1 and M2 but not M3, attenuated degradation (NT, Figure 8B). Thus, as is the case with other shuttle proteins, overexpression of ZNF216 inhibits degradation of unstable proteins via the UPS.

Discussion

ZNF216 is an atrogene

In this report, we show that *Znf216*$^{lex/lex}$ mice exhibit resistance to denervation-induced muscle atrophy. It has been